THE PENNSYLVANIA STATE UNIVERSITY
SCHREYER HONORS COLLEGE

DEPARTMENT OF BIOLOGY

THE ROLE OF PLANAR CELL POLARITY EFFECTOR GENE *INTURNED* IN HEDGEHOG SIGNALING, CILIOGENESIS, AND SKELETAL DEVELOPMENT IN MAMMALIAN EMBRYOGENESIS

RACHEL W. CHANG
SPRING 2013

A thesis
submitted in partial fulfillment
of the requirements
for a baccalaureate degree
in Biology
with honors in Biology

Reviewed and approved* by the following:

Aimin Liu
Associate Professor of Biology
Thesis Supervisor

Daniel Cosgrove
Professor of Biology
Honors Adviser

* Signatures are on file in the Schreyer Honors College

ABSTRACT

The coordinated interactions of molecular and cellular components during embryonic development are highly dependent upon the core developmental pathways. Among these pathways is Hedgehog (Hh) signaling. Hh signaling affects a variety of developmental processes, including body axis formation, neural and digit patterning, gonad development, cell proliferation, and bone ossification and growth. In mammals, the primary cilia, microtubule-based organelles on the surface of quiescent cells, are required for Hh signaling. To further explore the genetic basis of embryogenesis, we examined the *double-thumb* (*dtm*) mouse mutant of the *Inturned (Intu)* gene, a planar cell polarity (PCP) effector gene. PCP effector genes function downstream of PCP genes that are responsible for processes such as convergent extension and alignment of cilia in the cochlea. *Dtm* mutants carry a recessive, missense point mutation in *Intu* that results in decreased body size and survival, skeletal defects (mild polydactyly with one extra digit per limb, reduced and delayed ossification in the limbs and vertebrae, and misaligned ribs and sternal vertebrae), delayed neural patterning, and reduced ciliation in the kidney and ventral node. By characterizing the expression of a Hh pathway target, Patched1 (Ptch1), we found that Hh signaling is decreased during cartilage differentiation. These results suggest that *Intu* is important for both Indian Hedgehog (Ihh)-mediated bone ossification and Sonic Hedgehog (Shh)-mediated embryonic patterning, likely through regulating cilia formation. Such investigations into the genetic and molecular basis of ciliogenesis and skeletal development may have future clinical applications in the understanding and treatment of cilia-related ailments in humans.

Keywords: Hedgehog signaling, Indian Hedgehog signaling, Sonic Hedgehog signaling, planar cell polarity effector gene, polydactyly, primary cilia, ciliogenesis, Inturned, skeletal development, endochondral ossification

TABLE OF CONTENTS

LIST OF FIGURES

ACKNOWLEDGEMENTS

Thank you to Dr. Aimin Liu for his guidance, discussion, and suggestions throughout these studies and the preparation of the manuscript. Thank you to the members of the Liu laboratory – Huiqing Zeng, Jinling Liu, Xuan Ye, and Hongchen Cai – for their technical assistance. The time and feedback of Dr. Daniel Cosgrove is also much appreciated. Finally, much love and gratitude to my family – especially my parents, Cindy Ng and Dr. Gordon Chang – friends, and mentors for their ongoing support and encouragement in all my endeavors.

This research is generously supported by the Eberly College of Science of The Pennsylvania State University and the Polycystic Kidney Disease Foundation.

INTRODUCTION

Embryonic development is a complex process that requires coordinated interactions of molecular and cellular components under genetic control. This complexity is reflected in the diverse congenital syndromes resulting from disruptions of core developmental signaling pathways, including Wnt, Notch, FGF, TGFβ, and Hedgehog (Hh) (Arthur and Bamforth, 2011; Ignelzi et al., 2003; Loomes et al., 2007; Wu et al., 2011). Ciliopathies comprise one class of these developmental syndromes (Baker and Beales, 2009; Pan et al., 2005). Ciliopathies often present with combinations of severe facial or digital deformities, abnormal cognitive function and neural morphology, polycystic kidneys, and vision or hearing impairments (Baker and Beales, 2009; Louvi and Grove, 2011). The pathology is caused by insufficient primary cilia, microtubule-based cellular structures important for the localization of molecular components of Hh signaling (Baker and Beales, 2009). Examples of ciliopathies include Polycystic Kidney Disease (PKD, OMIM 173 900), Bardet-Biedl (BBS, OMIM 209 900), Joubert (JS, OMIM 213 300), Meckel (MKS, OMIM 24900), and Kartagener (OMIM 244 400) Syndromes (Baker and Beales, 2009; OMIM, 2013; Pan et al., 2005). Therefore, understanding the genetic and molecular basis of ciliogenesis and the role of Hh signaling in embryonic development, which we will explore here, is clinically relevant.

HEDGEHOG (Hh) SIGNALING

The Hedgehog (Hh) signaling pathway is essential for embryonic development, patterning, and growth. The Hh pathway functions in both invertebrates (such as fruit flies,

leeches, and sea urchins) and vertebrates (such as zebrafish, frogs, chickens, humans, rats, and mice) (Varjosalo and Taipale, 2008).

Hh signaling impacts development by regulating the temporal and spatial expression of developmental genes at the transcriptional level. While variations in the Hh pathway exist between species, the general scheme is similar **(Figure 1)**. Here, we will discuss the vertebrate pathway, the focus of our current study.

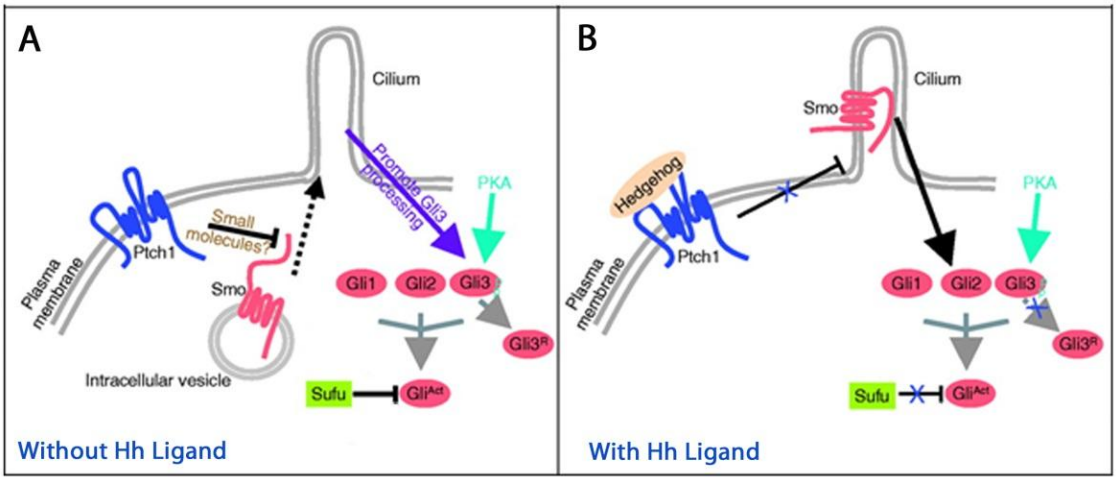

Figure 1 – Hh signaling pathway – (**A**) In the absence of Hh ligand, Patched1 (Ptch1) prevents the accumulation of Smoothened (Smo) in cilia, possibly through the action of a small molecule. Gli3 is phosphorylated by protein kinase A (PKA) and processed into a repressor form ($Gli3^R$) in a cilia-dependent manner. The activation of all Gli proteins is inhibited by Suppressor of Fused (Sufu). (**B**) In the presence of high levels of Hh ligand, Ptch1 inhibition is relieved; Smo is targeted to cilia and activates Gli proteins in a cilia-dependent manner. Gli3 processing is also inhibited. Figure and caption modified from Huangfu and Anderson, 2006.

Hh ligand binds to and deactivates Patched (Ptch), an Hh receptor (Pepinsky et al., 1998; Simpson et al., 2009). The deactivation of Ptch relieves the repression of the transmembrane protein Smoothened (Smo) (Simpson et al., 2009; Taipale et al., 2002). Activated Smo localizes to the primary cilia, preventing the phosphorylation and proteolytic processing of transcription factor proteins Gli1, Gli2, and Gli3 (Varjosalo and Taipale, 2008). Gli proteins in their full-length activator forms promote the transcription of Hh target genes; Gli proteins in their processed and truncated repressor forms inhibit transcription. In general, Gli1 and Gli2 serve as transcriptional activators and Gli3 as a transcriptional repressor.

In addition to changes in Ptch and Smo activity, other molecules can alter Gli levels and Hh target gene expression. For example, Rab23, a vesicular transport protein, affects the subcellular localization of pathway components downstream of Smo and upstream of Gli (Eggenschwiler et al., 2006; Eggenschwiler et al., 2001; Evans et al., 2003). This increases Gli3 repressor levels and decreases Gli2 activator levels. In addition, Suppressor of Fused (Sufu) protein inhibits Gli activity by interacting with the C- and N-terminal ends of Gli and sequestering it in the cytoplasm (Ding et al., 1999).

The widespread developmental effects of Hh signaling depend on the Hh gradient and the downstream gene expression patterns throughout embryogenesis (Briscoe and Ericson, 2001; Harfe et al., 2004). The functions of Hh signaling are achieved by three distinct types of Hh signaling – Sonic Hedgehog (Shh), Desert Hedgehog (Dhh), and Indian Hedgehog (Ihh).

Sonic Hedgehog (Shh) Signaling

Shh, perhaps the best-studied Hh family member, primarily affects cell proliferation, axis formation, and patterning in the nervous system and limb. Shh affects cell proliferation and survival by regulating cell proliferation genes. Among these are cell cycle regulators cyclins D and E and neuroblastoma-derived myelocytomatosis oncogene (N-myc) (Duman-Scheel et al., 2002; Kenney et al., 2003). N-myc not only regulates cell division and cancers in the brain and sensory-related structures (i.e. retina and optic nerve), but also those in the developing gut, kidney, lung, and limb (Brodeur et al., 1984; Dang, 2012; Garson et al., 1989; Jensen and Wallace, 1997; Lee et al., 1984; Stanton et al., 1992; Wallace and Raff, 1999; Zhou et al., 2011). These cancers, plus breast, pancreatic, and epithelial cancers, often result from somatic and germline mutations in *Ptch*, *Smo*, *Sufu*, and *Gli1* (Hahn et al., 1996; Johnson et al., 1996; Varjosalo and Taipale, 2008). N-myc is also important in maintaining the pluripotency of

embryonic stem cells and the multipotency of mammary and neuronal stem cells (Martinez-Cerdeno et al., 2012; Moumen et al., 2012; Varlakhanova et al., 2010).

During early development, Shh facilitates the establishment of the mesodermal dorsal/ventral axis (Gilbert, 2010). The mesoderm is the germ layer that gives rise to the notochord, musculoskeletal system, urogenital system, blood, and the vessel epithelia (Gilbert, 2010). For the development of the ventral axis, Shh upregulates bone morphogenic protein 4 (BMP4), a ventralizing factor (Harland, 1994; Winnier et al., 1995). The action of Shh on BMP4 is indirect. For example, vasculogenesis, one of the most ventral processes, requires BMP4 that is upregulated by the Shh-mediated expression of *Foxf1* in the mesoderm (Astorga and Carlsson, 2007).

In the developing neural tube, the decreasing ventral-to-dorsal Shh gradient activates and represses various class I and class II homeodomain transcription factors, respectively, in the ventral neural tube (Jacob and Briscoe, 2003; Meyer and Roelink, 2003) **(Figure 2)**. The subsequent antagonistic interactions among these transcription factors sharpens gene expression boundaries in the neural tube and promotes the differentiation of neuronal cells (Jacob and Briscoe, 2003). Due to its prevalence in mesoderm and neural tube patterning, loss of Shh function causes somite and neural tube defects (Chiang et al., 1996).

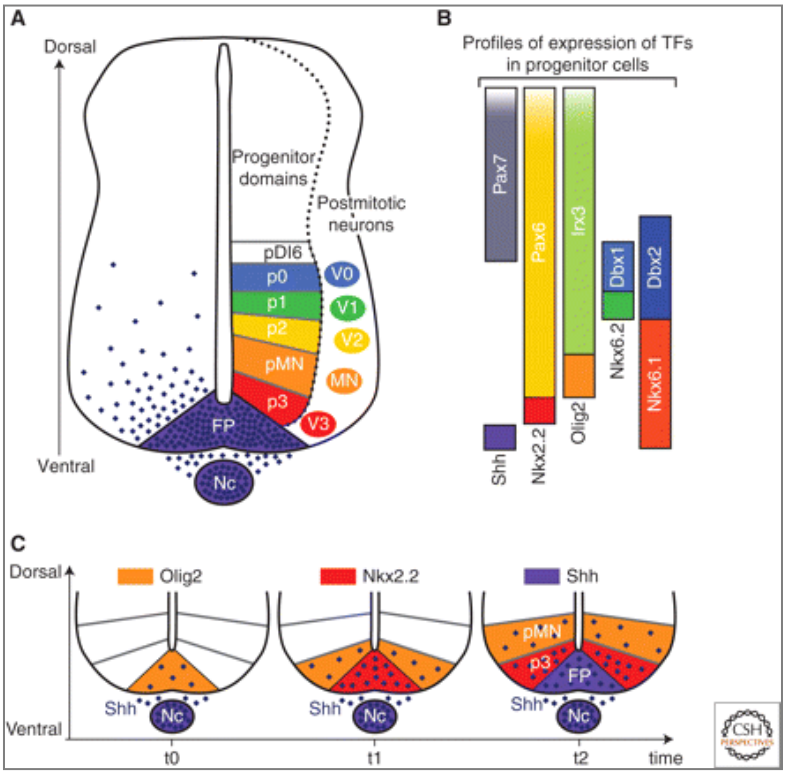

Figure 2 – Shh gradient affects expression of transcription factors (TFs) and determination of progenitor cells in the ventral neural tube – (A) Along the dorsal–ventral (D/V) axis of the ventral neural tube are six domains of progenitor cells, FP, p3, pMN, p2, p1, and p0, which generate V0–V3 and MN neuronal subtypes. The spatial organization of the progenitor domains is established by a gradient of Shh protein (purple) secreted from the notochord (Nc) and floor plate (FP). **(B)** The restricted expression profiles of the TFs Nkx2.2, Olig2, Nkx6.1, Nkx6.2, Dbx1, Dbx2, Irx3, Pax6, and Pax7 within progenitors is regulated by the Shh gradient. Each progenitor domain expresses a unique combination of TFs. **(C)** Olig2, Nkx2.2, and Shh distinguish the three most ventral progenitor domains, pMN, p3, and FP, respectively. The expression of each of these markers is initiated at successive developmental time points within the midline of the neural tube and extends dorsally with the appearance of the next marker at the midline. This series of gene induction events occurs in parallel to the accumulation and extension of the Shh gradient in the ventral neural tube. Figure and caption modified from Jacob and Briscoe, 2003.

In addition to ventral neural tube patterning, Shh plays a significant role in brain development. As part of its role in cell proliferation, Shh increases the thickness and size of the cerebral cortex by regulating the Gli3 activator to Gli3 repressor ratio and the apoptotic rate of neural progenitors and stem cells (Komada, 2012; Wilson et al., 2012). Brain morphology is also impacted by Shh. Shh inhibits the transcription factor *Pax6*, which allows the formation of two cranial hemispheres and eye fields (Chiang et al., 1996; Gilbert, 2010). Thus, reduced Shh leads to a single brain lobe and cyclopia (Ahlgren and Bronner-Fraser, 1999; Chiang et al., 1996; Gilbert, 2010). Shh also promotes the differentiation of neural progenitors (Komada, 2012). For example, Shh regulation of transcription factors Nkx2.1 and Gsh2 facilitates the development of

oligodendrocytes and interneurons responsive to γ-aminobutyric acid (GABA), a neurotransmitter (Corbin et al., 2003).

Similar to its role in the nervous system, Shh regulates axis determination and patterning in the limb. The anterior/posterior (thumb/pinky) axis of the limb is determined by Shh originating from the zone of polarizing activity (ZPA) in the posterior region of the limb bud (Gilbert, 2010). Shh, highest in concentration in the posterior region, is sufficient for inducing anterior/posterior polarity (Laufer et al., 1994; Lopezmartinez et al., 1995; Riddle et al., 1993). Shh beads implanted under the apical ectodermal ridge (AER) in the anterior region of the limb bud induce the same mirror-image digit duplication as ZPA transplants (Laufer et al., 1994; Lopezmartinez et al., 1995; Riddle et al., 1993).

Digit identity is also specified by the length of Shh exposure. Digit 1, the most anterior digit, develops independently of Shh (Tabin and McMahon, 2008). In the absence of Shh, only a single digit of either digit 1 or nonspecific identity forms (Litingtung et al., 2002; Tabin and McMahon, 2008). The formation of digits 2-5 depends on increasing exposure time from anterior to posterior (Harfe et al., 2004; Tabin and McMahon, 2008). This exposure time is determined by the Shh-regulated expression of BMP in the interdigital region posterior to a digit (Drossopoulou et al., 2000; Kawakami et al., 1996; Laufer et al., 1994). Thus, inhibiting BMP in an interdigital region transforms a digit to a more anterior identity (Drossopoulou et al., 2000; Kawakami et al., 1996; Laufer et al., 1994). In addition to digit identity, Shh also positively regulates the number of digits per limb (Litingtung et al., 2002). An overexpression of Shh can lead to polydactyly (Gilbert, 2010; Litingtung et al., 2002; Wang et al., 2011; Zeng et al., 2010). The requirement of Shh for proper digit identity and number is best revealed in experiments in which double mutants of *Shh* and *Gli3* exhibit polydactyly with digits of uniform identity (Litingtung et al., 2002; Ros et al., 2003; Scherz et al., 2007) **(Figure 3)**.

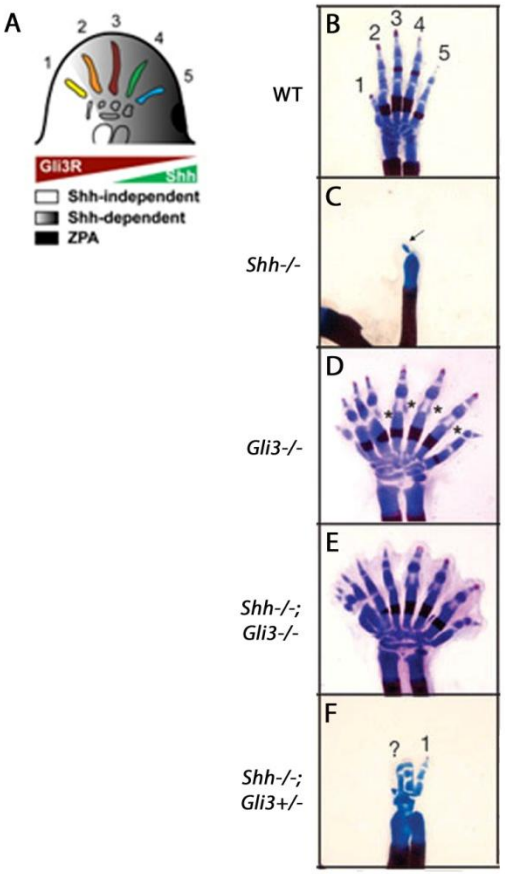

Figure 3 – Shh functions in establishing anterior/posterior (A/P) digit identity and digit number – (A) The Shh gradient in the zone of polarizing activity (ZPA) of the limb bud increases from anterior to posterior (digit 1/thumb to digit 5/pinky); Gli3 repressor (Gli3R) increases from posterior to anterior. The formation of the identity of digit 1 is independent of Shh, while the identities of all other digits depend on the Shh and Gli3R gradient. Figure from Bowers et al., 2012. **(B)** A wild type (WT) mouse forelimb. **(C)** A *Shh-/-* mouse limb with a single, unidentified digit. **(D)** A *Gli3-/-* mouse limb with polydactyly, reduced A/P digit identity, and gaps of unstained cartilage (*). **(E)** A *Shh-/-; Gli3-/-* mouse limb with polydactyly, reduced digit identity, gaps of unstained cartilage, bunching of the anterior digits, and kinking of the posteriormost digit. The minor differences between **D** and **E** are not significant. **(F)** A *Shh-/-; Gli3+/-* mouse limb with three or four digits. All unfused digits are of digit 1 identity, regardless of A/P position. Figures **B-F** show mouse forelimbs at E16.5. Figures and captions modified from Litingtung et al., 2002.

Shh is also involved in vasculogenesis and angiogenesis. Shh regulates the transcription of fibroblastic growth factor 4 (FGF4) and vascular endothelial growth factor A (VEGF-A) in hypoxic conditions that stimulate embryonic blood vessel development (Gerhardt et al., 2003; Pola et al., 2001).

Desert Hedgehog (Dhh) Signaling

The second Hh family member, Dhh, is primarily involved in gonad and germ cell development (Clark et al., 2000; Wijgerde et al., 2005). In males, Dhh is required for testis development and the differentiation of testicular cells (Bitgood et al., 1996; Clark et al., 2000; Pierucci-Alves et al., 2001; Yao et al., 2002). *Dhh* null males lack testosterone-secreting Leydig

cells and possess abnormal seminiferous tubules, Sertoli cells, and testicular cords (Clark et al., 2000; Pierucci-Alves et al., 2001). These reproductive components are involved in producing, nourishing, and transporting sperm cells, respectively (Gilbert, 2010). Therefore, *Dhh* null individuals lack mature sperm and may exhibit germ cells located outside the testicular cords (Bitgood et al., 1996; Clark et al., 2000; Pierucci-Alves et al., 2001).

In females, Dhh is found in the ovarian follicles in theca cells and their precursors (Wijgerde et al., 2005). Theca cells are endocrine follicular cells responsible for producing the chemical precursors for estrogen biosynthesis (Magoffin, 2005). Thus, *Dhh* mutant females often exhibit immature theca cells and fertility issues (Magoffin, 2005; Spicer et al., 2009).

In the nervous system, Dhh promotes the development of Schwann cells, supporting cells of the peripheral nervous system that protect neurons and aid in saltatory signal transduction (Kuspert et al., 2012; Smith et al., 2001). Dhh affects the collagen content, thickness, tight junctions, and basal lamina uniformity of the perineurium, the protective sheath around each Schwann cell (Parmantier et al., 1999).

In addition to its roles in the reproductive and nervous systems, Dhh has been implicated in the maintenance and regeneration of corneal cells via wound healing mechanisms (Kucerova et al., 2012; Saika et al., 2004). Dhh negatively regulates erythropoietic stem cell and pancreatic β-cell differentiation as well (Lau et al., 2012; Mfopou et al., 2012).

Indian Hedgehog (Ihh) Signaling

The third Hh family member, Ihh, has been most widely studied in the context of endochondral ossification. Endochondral ossification is the process by which ribs, vertebrae, and long bones of the limbs calcify and grow through the replacement of cartilage by bone (Lai and Mitchell, 2005) **(Figure 4** and **Figure 5)**.

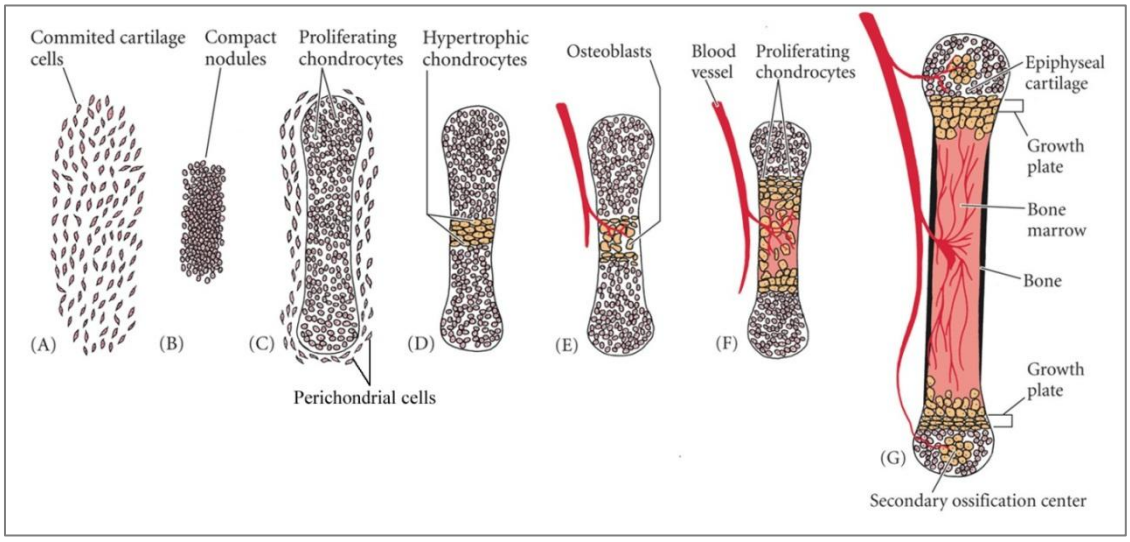

Figure 4 – The endochondral ossification process – (A-C) Mesenchymal cells determined to become chondrocytes will form compact nodules in the center of the cell mass and subsequently become proliferating chondrocytes. Cells on the periphery will become perichondrial cells around the developing cartilage. **(D)** Once cell division ceases, proliferating chondrocytes hypertrophy. **(E-F)** As chondrocytes hypertrophy, intercellular signaling promotes vascularization, which allows for the invasion of osteoblasts and the replacement of cartilage by bony matrix. **(G)** Ossification continues toward the ends of the bone until the growth plate fuses with the secondary ossification center. Bone lengthening is complete. Figure from Gilbert, 2006.

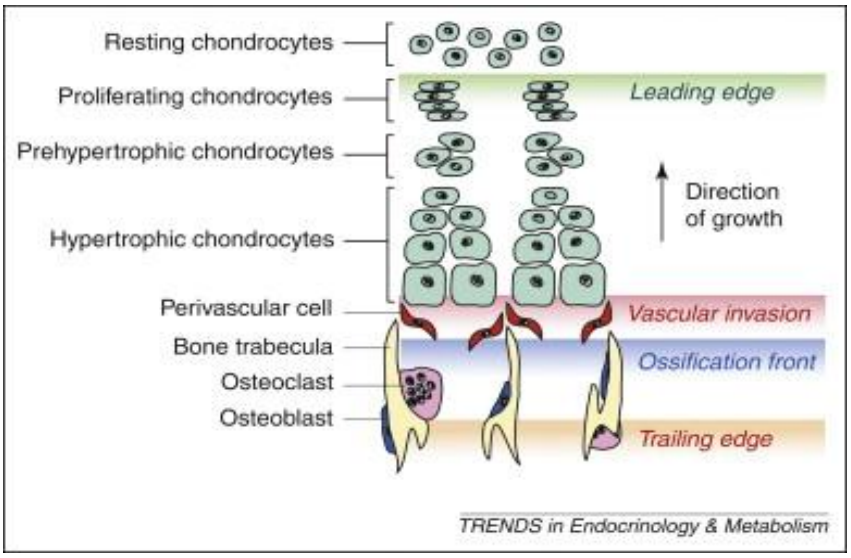

Figure 5 – Growth plate structure – Cells at different stages of differentiation that play different roles in endochondral ossification are identified on the left. The growth plate is dynamic with a leading edge (green) where chondrocytes proliferate and a trailing edge (brown) where the cartilage template is degraded by invading vascular cells (red). Chondrocytes are replaced by the expanding ossification front (blue). Figure and caption modified from Horton and Degnin, 2009.

Bone development begins with the condensation of mesenchymal cells **(Figure 4A-B)**. The cells in the center of the cell mass differentiate into cartilaginous cells known as chondrocytes. Cells in the periphery of the cell mass develop into the perichondrium, the sheath

surrounding the developing cartilage. The chondrocytes, which form the growth plate **(Figure 5)**, divide and secrete cartilaginous extracellular matrix (ECM) in the central area of the developing bone known as the proliferative zone **(Figure 4C)**. In mice, cartilage formation begins at stage E11.5. The chondrocytes become prehypertrophic chondrocytes once cell division ceases. Prehypertrophic chondrocytes differentiate into collagen-secreting hypertrophic chondrocytes, forming the hypertrophic zone **(Figure 4D)**. As the chondrocytes hypertrophy, interactions between the cartilaginous ECM and growth factors promote vascularization of the region. Vascularization permits the invasion of osteoblasts, the bone-forming cells **(Figure 4E)**. This occurs at approximately stage E13.5-E14.5 in mice. As the osteoblasts deposit bony matrix, the hypertrophic chondrocytes undergo apoptosis and are replaced by bone. The chondrocytes near the perichondrium are replaced by osteoblasts that form the periosteum, the vascularized sheath around a mature bone. The replacement of the cartilage in the primary ossification center in the diaphysis (shaft) of the bone continues toward the epiphyses (ends) of the bones where cartilage is being added at the growth plate **(Figure 4F-G)**. The ossification of the expanding cartilage framework causes bone lengthening. Simultaneously, the cartilage in the epiphyses, known as the secondary ossification centers, undergoes replacement by bone. Once the primary ossification center, growth plate, and secondary ossification center fuse and are completely ossified, bone lengthening is complete (Young et al., 2006).

Ihh indirectly mediates chondrocyte proliferation and ossification **(Figure 6)**.

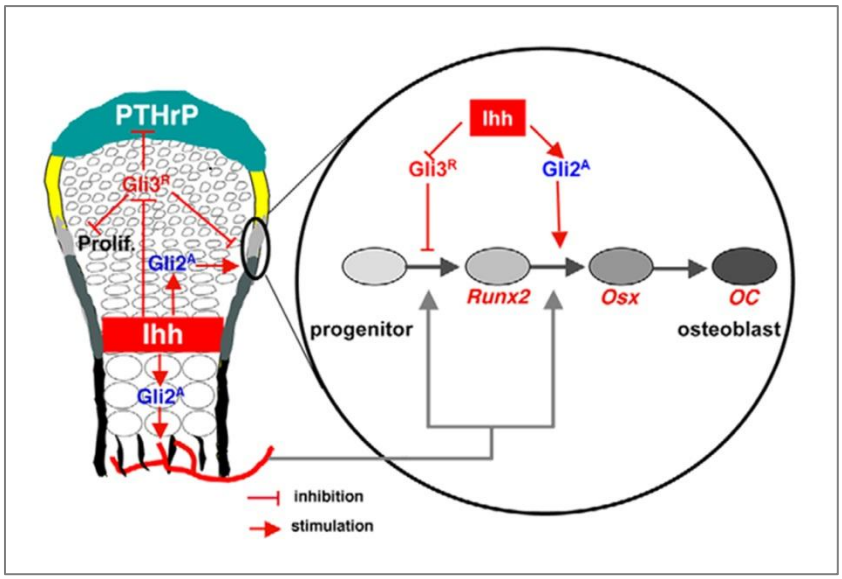

Figure 6 – Ihh promotes chondrocyte proliferation and osteoblast differentiation – Ihh indirectly promotes chondrocyte proliferation by relieving the repression on parathyroid hormone related protein (PTHrP) by Gli3 repressor ($Gli3^R$). PTHrP maintains chondrocytes in a proliferative stage and prevents premature hypertrophy. Ihh promotes osteoblast differentiation by repressing $Gli3^R$ and activating Gli2 activator ($Gli2^A$). This allows for the expression of osteogenesis master regulator *Runx2*. $Gli2^A$ induces vascularization needed for osteoblast differentiation. $Gli2^A$ facilitates the expression of osteoblast-related transcription factors and secretions, such as osterix *(osx)* and osteocalcin (oc). Gli1, not shown, functions in early differentiation (Hojo et al., 2012). Figure from Jeong and Long, 2009.

Ihh, upregulated by BMP and retinoic acid, positively regulates the rate of chondrogenesis and chondrocyte hypertrophy by repressing Gli3 repressor (Joeng and Long, 2009; Minina et al., 2002; St-Jacques et al., 1999; Vortkamp et al., 1996; Yoon and Lyons, 2004; Yoshida et al., 2001). Decreasing Gli3 repressor activity activates parathyroid hormone-related protein (PTHrP) (Karp et al., 2000; Lai and Mitchell, 2005). PTHrP maintains chondrocyte proliferation and delays chondrocyte hypertrophy by downregulating Ihh via a negative feedback loop (Macica et al., 2011). Disruption of the feedback mechanism often results in stunted growth (Hellemans et al., 2003; Karp et al., 2000; Maeda et al., 2007; Razzaque et al., 2005; St-Jacques et al., 1999). This is due to the premature termination of chondrocyte proliferation and the premature initiation of chondrocyte hypertrophy (St-Jacques et al., 1999). While the Ihh/PTHrP feedback mechanism is the primary regulator of embryonic chondrocyte development, PTHrP-

independent Ihh promotion of chondrocyte hypertrophy is more prevalent postnatally (Mak et al., 2008b)

Ihh repression of the Gli3 repressor and activation of Gli2 also activate the master regulator transcription factor Runx2, promoting osteoblast differentiation (Inada et al., 1999; Joeng and Long, 2009; Komori, 2011; Maruyama et al., 2007; Shimoyama et al., 2007). Runx2 facilitates the expression of transcription factors and bony matrix components secreted by osteoblasts, including osterix, alkaline phosphatase, and osteocalcin (Shimoyama et al., 2007). In addition, Runx2 and Gli2 promote the vascularization required for osteoblast differentiation (Joeng and Long, 2009; Komori, 2011; Liu et al., 2002). Although upregulation of Gli2 is sufficient for vascularization in the absence of Ihh, osteoblast differentiation cannot occur in the presence of Gli3 repressor (Joeng and Long, 2009).

Studies of markers at various stages of osteoblast differentiation show that Gli1 can induce early osteoblast differentiation even in the absence of Runx2 (Hojo et al., 2012). Gli1 and Gli2 are redundant in function, as *Gli1;Gli2* double mutants exhibit bone development delays while single mutants are unaffected (Hojo et al., 2012).

In addition to endochondral ossification, Ihh contributes to neural crest formation, intestinal smooth muscle and ovarian follicle cell development, pancreatic β-cell differentiation, erythropoiesis, and bone resorption (Aguero et al., 2012; Cridland et al., 2009; Dyer et al., 2001; Mak et al., 2008a; Mfopou et al., 2012; van den Brink, 2007; Wijgerde et al., 2005; Zacharias et al., 2011).

Figure 7 summarizes the role of Hh signaling throughout murine embryogenesis.

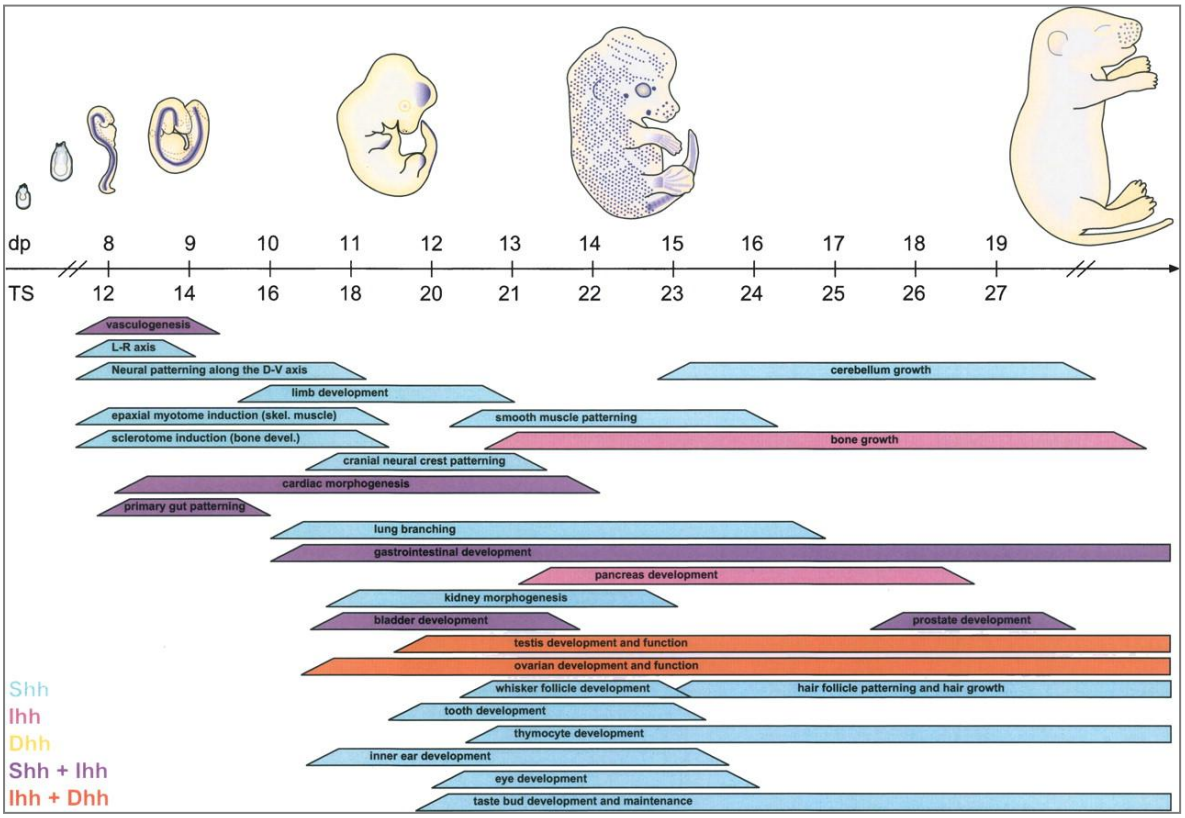

Figure 7 – Shh, Ihh, and Dhh affect multiple organ systems during murine embryonic development – Timeline scale: days post conception (dp) and Theiler Stage (TS). Figure from Varjosalo and Taipale, 2008.

PRIMARY CILIA

The intracellular transduction of mammalian Hh signaling depends on the primary cilia, non-motile, microtubule-based organelles present on the cell surface of most quiescent vertebrate cells (Louvi and Grove, 2011; Simpson et al., 2009) **(Figure 8)**. The axoneme (core) of each primary cilium contains nine pairs of microtubules in a 9+0 arrangement and is anchored to the ciliary basal body (Simpson et al., 2009) **(Figure 8A)**.

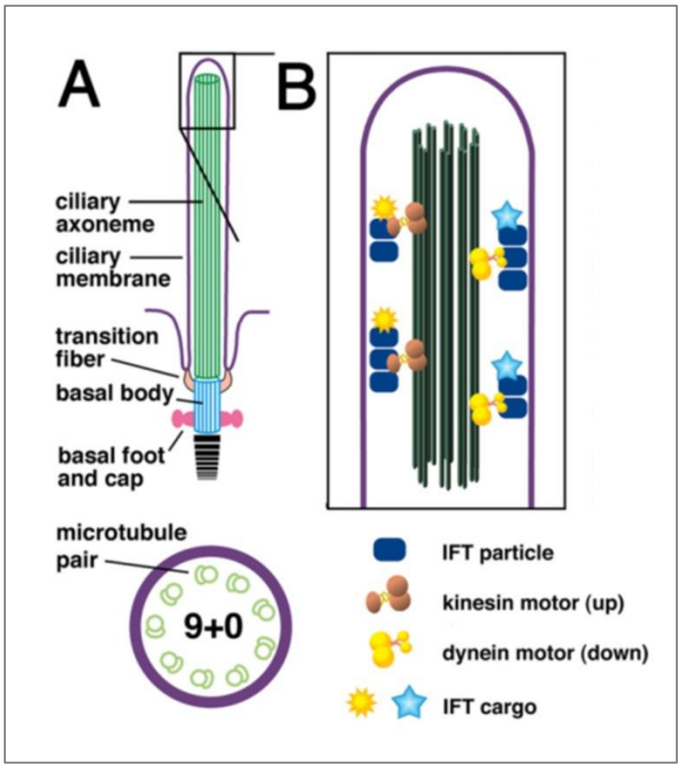

Figure 8 – Primary cilia structure and components – (A) The exterior components and structure of a primary cilium and the 9+0 arrangement of the microtubules in the axoneme. **(B)** The intraflagellar transport (IFT) particles and motor proteins that move materials required for ciliogenesis and signaling to the tip (anterograde IFT) and to the base (retrograde IFT) of the cilium. Figure from Louvi and Grove, 2011.

Ciliogenesis requires the transport of materials between the basal body and the tip of the cilium during interphase of the cell cycle (Louvi and Grove, 2011; Simpson et al., 2009) **(Figure 8B)**. Eleven Complex B intraflagellar transport (IFT) proteins and kinesin-2 motor proteins transport materials to the tip of cilia in a process known as anterograde IFT (Louvi and Grove, 2011; Simpson et al., 2009). In contrast, materials are transported from the tip to the basal body by six Complex A IFT proteins and Dynein motor proteins during retrograde IFT (Louvi and

Grove, 2011; Simpson et al., 2009). Among the transport proteins involved, some IFT-B and Kinesin proteins are required for ciliogenesis (Simpson et al., 2009). Examples include Ift88, Ift172, and Kinesin motor protein Kif3a (Huangfu et al., 2003; Park et al., 2006).

The Role of the Cilia in Signal Transduction

The primary cilia are required for Hh signal transduction in mammals (Goetz and Anderson, 2010; Zeng et al., 2010). In the absence of Hh signaling, Ptch in the cilia prevents the ciliary localization of Smo (Rohatgi et al., 2007) **(Figure 1A)**. In the presence of Hh signaling, the ciliary localization of Smo promotes the localization of unprocessed Gli and Sufu at the tip of the cilia and the subsequent activation of Gli proteins (Corbit et al., 2005; Haycraft et al., 2005; Rohatgi et al., 2007) **(Figure 1B)**.

IFT-associated ciliary proteins have also been found to affect the cleavage of Gli proteins to form Gli repressors (Haycraft et al., 2005; Huangfu and Anderson, 2005; Huangfu et al., 2003; Liu et al., 2005). This role of cilia is indicated by studies in which *Ift88* mutant limb bud cells exhibited an elevated ratio of full-length Gli3 to Gli3 repressor levels *in vitro* and polydactyly reminiscent of *Gli3* mutants *in vivo* (Haycraft et al., 2005). In addition, Kinesin motor proteins of the cilia have been implicated in the release of Gli3 from Sufu, freeing Gli3 to act on the target gene (Humke et al., 2010). While these studies support involvement of ciliary proteins in regulating Gli activity, it remains unclear whether the regulation occurs directly or indirectly through the maintenance of cilia.

PLANAR CELL POLARITY (PCP) AND PCP EFFECTOR GENES

Planar cell polarity (PCP) is the organization and alignment of tissues and repetitive structures along an axis in a single plane (Eaton and Julicher, 2011; Rida and Chen, 2009; Wallingford and Mitchell, 2011) . One of the best-studied PCP processes is convergent extension

(CE) (Keller, 2002). During CE, an embryo elongates head to tail through cells moving toward and intercalating along the mediolateral axis. Therefore, PCP mutants characteristically present with defects in CE, neural tube closure, and axon tract formation (Tissir and Goffinet, 2010; Wang et al., 2006). PCP genes affect these processes by downregulating Wnt signaling, one of the core developmental signaling pathways involved in axis determination and limb development (Corbit et al., 2008; Wallingford and Mitchell, 2011).

PCP genes, which include *Frizzled (Fz), Van Gogh (Vang), Disheveled (Dsh), Flamingo (Fmi), Diego (Dgo),* and *Prickle (Pk),* also facilitate the development of cilia and mechanosensory hairs of the inner ear (Rida and Chen, 2009; Ross et al., 2005; Wallingford and Mitchell, 2011; Wang et al., 2006). The connection between cilia and PCP has been demonstrated in multiple studies. Not only do ciliary gene knockout mice show defective epithelial PCP, but mouse models of Bardet-Biedl Syndrome (BBS), a ciliopathy, also exhibit interactions between ciliary and PCP proteins (Jones et al., 2008; Ross et al., 2005).

The PCP effector genes function downstream of the core PCP genes (Rida and Chen, 2009). They utilize the directional information generated by the asymmetrically localized PCP proteins and facilitate tissue-specific morphological cell polarity changes (Jones and Chen, 2007; Tree et al., 2002). The PCP effectors include *Fuzzy (Fy), Fritz,* and *Inturned (Intu),* the latter of which is the focus of our current study (Collier et al., 2005; Heydeck and Liu, 2011).

Inturned (Intu)

Intu homologs exist in multiple species, including *Drosophila, Xenopus,* mouse, rat, and human (Park, 2008; Park et al., 2006; Zeng et al., 2010).

Drosophila Intu (*DIntu*) plays a role in the number/initiation and polarity of wing hairs, important sensory organelles (Wong and Adler, 1993). Each region of the wing typically displays uniformly oriented (polarized) hairs with one hair per cell (Wong and Adler, 1993). The majority

of wing cells of *DIntu*$^{-/-}$ mutants possesses two wing hairs, even in the presence of an adjacent wild type cell. This suggests that *DIntu* cell-autonomously inhibits wing hair initiation, though not in a fully penetrant manner (Park et al., 1996). However, *DIntu* does not regulate wing hair development alone. For example, co-immunoprecipitation, localization, and fusion protein rescue studies show that DIntu interacts with and recruits other tissue polarity proteins, including multiple wing hair (mwh) (Lu et al., 2010).

Xenopus Intu (*XIntu)* is involved in ciliogenesis and PCP processes (Park et al., 2006). Morpholino knockdown of *XIntu* results in neural tube defects associated with faulty CE and fewer and abnormally oriented cilia (Park et al., 2006). In addition, XIntu co-localizes with PCP-associated Wnt pathway regulator Disheveled (Dsh) at the apical surface of ciliated cells but not non-ciliated cells (Park et al., 2006). These observations support the involvement of *XIntu* in PCP. *XIntu* mutants also display craniofacial, maxillary, eye, and brain morphology defects reminiscent of those observed in other known Hh pathway mutants (Park et al., 2006). These observations suggest that *XIntu* mediates Hh signaling as well.

Mouse *Intu* (*mIntu*), 72% similar to the XIntu protein and 42% similar to the DIntu protein, is important in Hh-mediated processes (Zeng et al., 2010). Our lab previously showed that *mIntu* is important in digit, brain, and neural tube patterning and ciliogenesis (Zeng et al., 2010). *Intu* null mutants exhibit severe polydactyly of up to nine digits, disproportionate and malformed regions of the brain, and reduced cilia number and length. The severe developmental defects consistent with disrupted Hh signaling cause lethality in all embryos by E16.5. However, mutant mice exhibit only mild CE-related defects. These observations indicate that *mIntu* either has little to no role in mammalian PCP or its role in PCP is functionally redundant to those of other PCP or PCP effector genes. Our lab subsequently showed that *Fy* and *mIntu* are not functionally redundant (Heydeck and Liu, 2011).

Double Thumb (Dtm) Mutant

In order to further investigate the role of *Intu* in mammalian development, we studied a mouse mutant called *double-thumb* (*dtm*, also referred to as $Intu^{dtm}$) for the duplication of digit 1 in all four limbs (Liu, unpublished) **(Figure 9)**. *Dtm* mice possess a nonsynonymous T to A base substitution in a highly conserved region of the *Intu* gene located on chromosome 3 **(Figure 9A-C)**. The substitution results in the replacement of a hydrophobic amino acid isoleucine with a polar amino acid asparagine near the C-terminal end of the 942-amino acid Intu protein **(Figure 9B, D)**. This change results in a recessive allele **(Figure 9E)**.

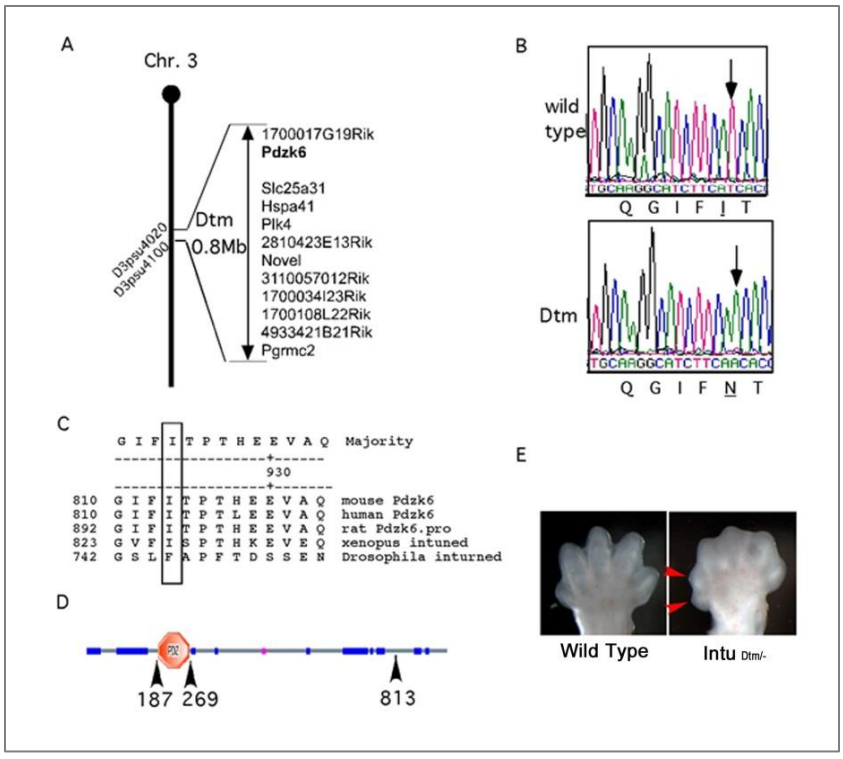

Figure 9 – Genetic overview of the *double thumb* (*dtm*) mutant – (A) The *dtm* mutation of the 0.8Mb long *Inturned (Intu)* gene, also known as *Pdzk6*, is located on chromosome 3 in a region containing other genes shown. **(B)** The *dtm* mutation is a nonsynonymous point mutation that causes an amino acid change from isoleucine (I) to asparagine (N) (arrow). **(C)** The *dtm* mutation is found in a highly conserved region of Intu. **(D)** The *dtm* mutation occurs at amino acid 813. The PDZ domain, a protein binding domain, occurs between amino acid 187 and 269. **(E)** The *dtm* mutation is a recessive allele, as indicated by the two thumbs (arrows) present in the $Intu^{Dtm/-}$ mice.

The goals of our present study are to characterize the *dtm* phenotype and to explore the underlying molecular causes of the observed phenotype. Based on the Hh signaling and ciliary defects of *Intu* null mutants and the role of Ihh in skeletal development, we hypothesize that the *dtm* mutation affects skeletal development and ciliogenesis. Here we report that *dtm* mutants

exhibit reduced survival and stunted growth, in addition to several skeletal, ciliary, and Hh-related characteristics. *Dtm* mutants display mild polydactyly, misaligned ribs, reduced ossification in the digits, forelimb bones, and vertebrae, and diminished Ptch1 expression in the forelimb bones. *Dtm* mutants also show delayed spinal cord patterning and reduced ciliation in the ventral node and kidney. *In vitro* ciliation studies, though preliminary, suggest that the $Intu^{dtm}$ protein cannot fully rescue the ciliation defects of *Intu* null mutant cells.

RESULTS

Dtm mice exhibit reduced survival

To determine the impact of the *dtm* mutation on viability and development, we monitored several litters from birth to postnatal week (PW) 4 **(Figure 10)**. All phenotypically wild type mice (true wild type and heterozygous individuals, referred to as "wild type" hereafter) survived to the end of the observation period. In contrast, only 55.5% of the *dtm* mice survived to PW1. The *dtm* mice experienced additional mortality between PW1 and PW2, which was not as severe as that between PW0 and PW1. By PW2, only 36.4% of the *dtm* mice remained. No additional mortality was observed among the *dtm* individuals in PW3 or PW4. The greater mortality observed in *dtm* mice than their wild type counterparts suggests an important role for *Intu* in the postnatal survival of the mice.

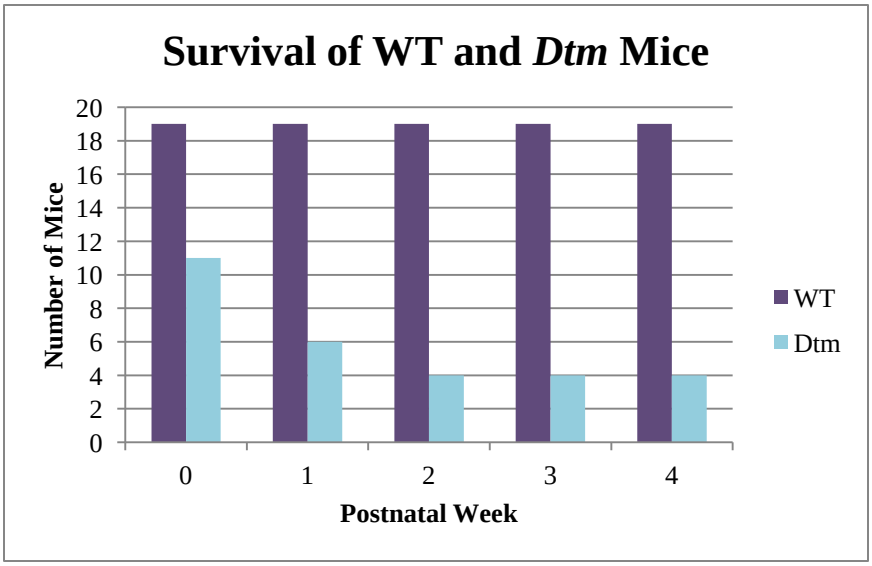

Figure 10 – *Dtm* mice exhibit reduced survival – *Dtm* mice exhibit mortality between postnatal week (PW) 0 and PW4 whereas wild type mice do not.

The reduction in viability indicates that the *dtm* mutation causes detrimental prenatal and/or postnatal abnormalities. The high mortality observed in the first two weeks followed by little to no mortality among the *dtm* mice suggests that these abnormalities may vary in severity. The mutation likely causes severe effects incompatible with long-term survival in individuals who die shortly after birth. It is also possible that severely affected individuals die during gestation. In contrast, the mutation likely causes milder defects that have little impact on survival in those who survive beyond the first two weeks.

Dtm mice exhibit reduced postnatal body size and weight

We noticed that the *dtm* mutants are consistently smaller than their wild type littermates, suggesting that *Intu* may play a role in regulating postnatal growth **(Figure 11A)**. To confirm and quantify this phenotype, we monitored the body weight of the pups from birth to six weeks **(Figure 11B)**. At birth, *dtm* mice (1.29g) weighed an average of 18.4% less than wild type mice (1.58g), a highly significant difference (p=0.0007). The body weights subsequently diverged through all time points for which data was collected. By PW6, *dtm* mice weighed 32% less than their wild type counterparts. The presence of significant weight differences at birth suggests that the *dtm* mutation affects prenatal development. The increasing divergence and statistically significant weight differences at PW2 (p=0.0023), PW3 (p=0.0341), and PW4 (p=0.0079) suggest that the prenatal changes have persisting postnatal effects. It is also possible that additional detrimental defects arise postnatally. We also observed clear differences at PW5 (p=0.0558) and PW6 (p=0.0566) in weight and size **(Figure 11A)**, but the small sample size of *dtm* mice likely affected the statistical analysis.

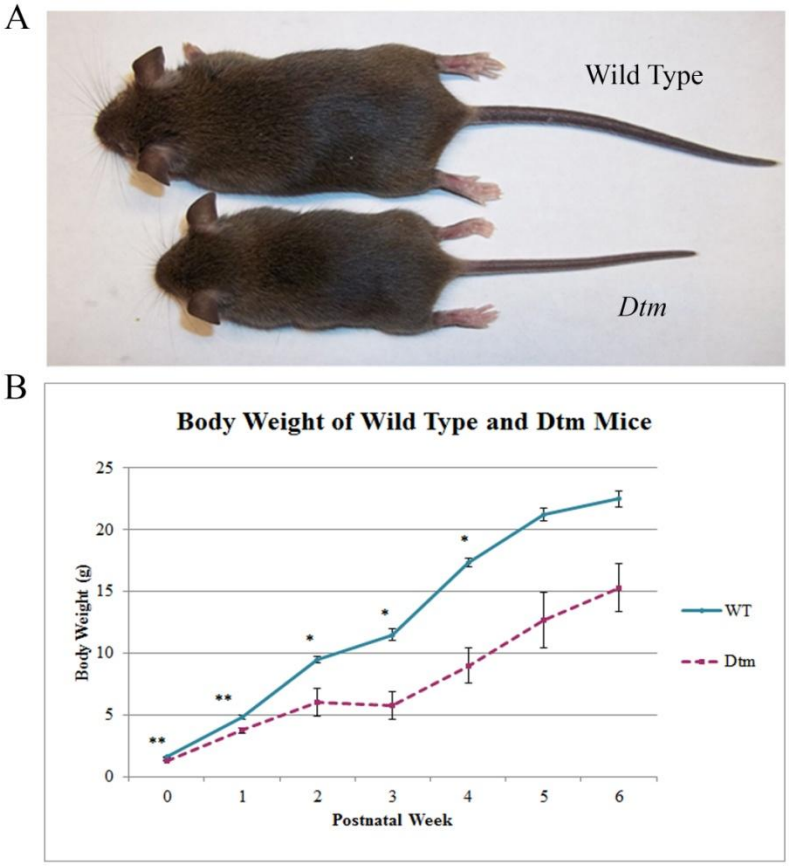

Figure 11 – *Dtm* mice exhibit reduced postnatal body size and weight – (A) PW6 littermates differ in size. **(B)** Body weights of wild type and *dtm* mice diverge from birth to PW6. *p<0.05; **p<0.005

SKELETAL CHARACTERISTICS

The lower body weight in *dtm* mice may result from defects in skeletal development. To address this possibility, we examined skeletal patterning and ossification in *dtm* mutants.

Dtm mutants likely exhibit forelimb bones of normal length in embryogenesis

One component of skeletal development we evaluated was the length of the forelimb long bones. Although wild type and *dtm* mice differed noticeably in postnatal size, no significant differences in forelimb bone lengths were observed at E16.5, E17.5, or E18.5 **(Figure 12)**. The bone lengths of the *dtm* individuals were nearly 100% of the wild type lengths. Minor deviations from wild type lengths are likely attributable to small sample size and methods of measurement.

These explanations may also account for the statistically significant value at E17.5 that is inconsistent with the rest of the data set.

The similar bone lengths of the wild type and mutant mice at embryonic stages are consistent with the similar birth size and small absolute difference in birth weight. It is likely that the difference in growth primarily occurs postnatally, as supported by the significant divergence in body weights **(Figure 11)**.

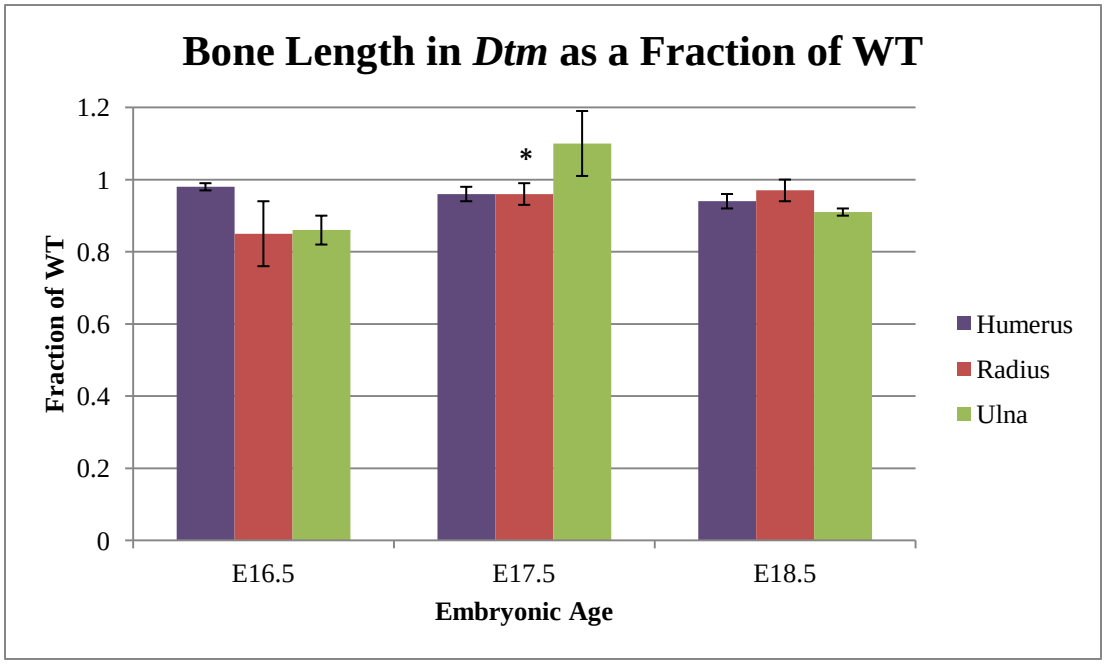

Figure 12 – *Dtm* mutants likely exhibit normal forelimb bone lengths during embryogenesis – The lengths of the *dtm* humerus, radius, and ulna are similar to the lengths of wild type counterparts except for the radius at E17.5. The significant difference (*) may be due to small sample size. *p<0.05

Dtm embryos exhibit reduced and possibly delayed digital and vertebral ossification

Although the lengths of the long bones are similar between wild type and *dtm* mutant embryos, we noticed an obvious delay in endochondral ossification in *dtm* mutants. Fewer domains of ossification were present in the digits of *dtm* mutants than wild type individuals at all three embryonic stages studied **(Figure 13A-F).** Since the reduced ossification did not resolve by

E18.5, it is possible that *dtm* individuals either have permanently less ossification than wild type or experience delays in ossification that resolve at a later time point.

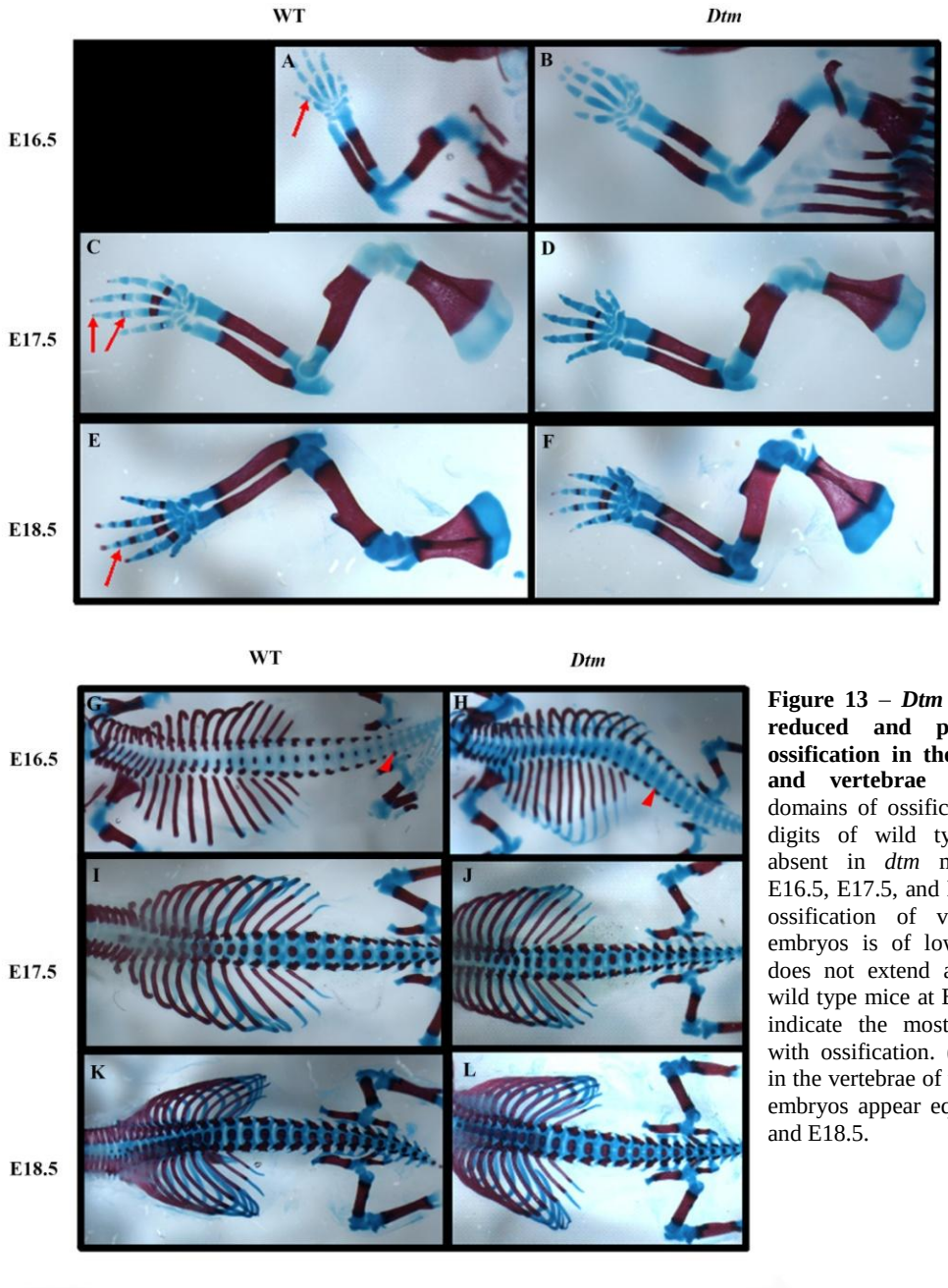

Figure 13 – *Dtm* embryos exhibit reduced and possibly delayed ossification in the forelimb digits and vertebrae – (A-F) Some domains of ossification (red) in the digits of wild type embryos are absent in *dtm* mice (arrows) at E16.5, E17.5, and E18.5. **(G-H)** The ossification of vertebrae of *dtm* embryos is of lower intensity and does not extend as caudally as in wild type mice at E16.5. Red arrows indicate the most caudal vertebra with ossification. **(I-L)** Ossification in the vertebrae of wild type and *dtm* embryos appear equivalent at E17.5 and E18.5.

We also observed a lower intensity and extent of ossification in the center of the vertebrae of *dtm* individuals than in wild type at E16.5 **(Figure 13G-H).** In wild type embryos, the vertebral ossification was very dark and extended caudally along the vertebral column to the pelvic level. In *dtm* mutants, the ossified region was lighter in color, smaller in size, and extended caudally only a few vertebrae beyond the rib cage. By E17.5 and E18.5, the ossification patterns were of equal intensity and extended along the length of the tail in both wild type and mutant individuals **(Figure 13I-L)**. The resolution of the ossification differences suggests that the *dtm* mutation may cause a delay in vertebral ossification.

Dtm embryos exhibit delayed ossification in forelimb bones at early stages

In addition to the ossification of the digits and vertebrae, we quantified the ossification in the forelimb bones as a fraction of bone length **(Figure 14)**. Significant differences in ossification between wild type and *dtm* individuals were consistently present at early time points, but generally absent at later time points. At E16.5, the ossified fraction of the humerus, radius, and ulna was significantly less in the mutants than in the wild type ($p=0.01$, 0.03, and 0.01, respectively). A 32%, 11%, and 8.3% difference in average ossified fraction of the humerus, radius, and ulna was observed, respectively. At E17.5, a significant difference was observed in the humerus (11% difference, $p=0.04$), but not in the radius or ulna (9.7% difference, $p=0.36$ and 3.3% difference, $p=0.27$, respectively). At E18.5, significantly less ossification was found in the radius of *dtm* embryos than in wild type (9.9% difference, $p=0.002$), but not in the humerus or ulna (1.6% difference, $p=0.41$ and 0% difference, $p=0.80$, respectively). The greater similarity in ossification at later stages suggests that the *dtm* mutation may cause ossification delays in the long bones of the forelimb. Similar delays in ossification were observed in the vertebrae, where less ossification was observed in the mutants at E16.5, but equivalent ossification was observed between wild type and mutant embryos at E17.5 and E18.5 **(Figure 13G-L).**

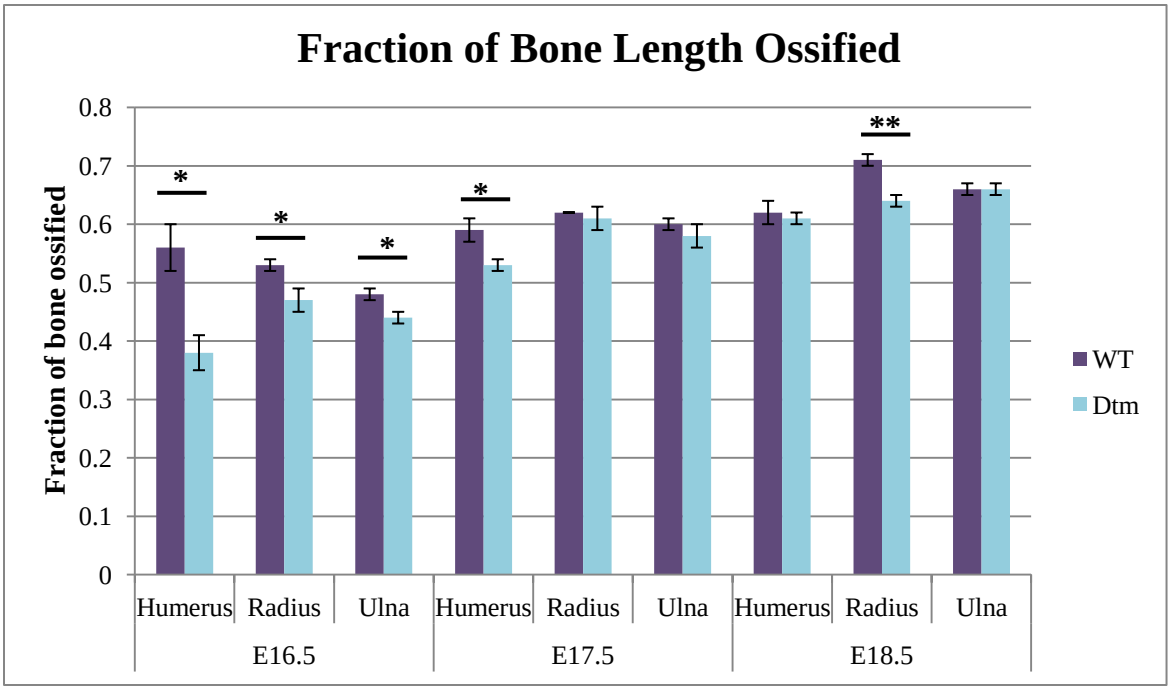

Figure 14 – *Dtm* embryos exhibit reduced ossification in the forelimb at early developmental stages – The fraction of the length of the humerus, radius, and ulna that is ossified is generally less in *dtm* mutants than in wild type at early stages, but equivalent at later stages. *p<0.05, **p<0.005

Dtm embryos exhibit reduced *Ptch1* expression in the forelimb bones

Previous studies indicate that Ihh promotes chondrocyte proliferation and hypertrophy during endochondral bone development (Joeng and Long, 2009). To investigate whether defective Hh signaling underlies the observed skeletal phenotype, we examined the expression of a direct target of Hh, *Ptch1*, via X-gal staining of mouse embryos expressing a *Ptch1-lacZ* reporter gene **(Figure 15)**. As previously reported, *Ptch1* is highly expressed in the perichondrium (a layer of cells surrounding the cartilage) and in the proliferative and hypertrophic chondrocytes near the ends of the bones.

In *dtm* mutant embryos **(Figure 15B, D, F)**, the level of *Ptch1* expression is lower compared to that in wild type embryos **(Figure 15A, C, E)**, suggesting reduced Hh signaling in *dtm* mutants. The reduced levels of *Ptch1* expression in *dtm* embryos at E14.5 support the notion

that the *dtm* mutation affects bone development in the earlier stages of ossification, which begins at around E13.5-E14.5. These results are consistent with the later stage (E17.5-E18.5) resolution of earlier stage (E16.5) ossification differences in the vertebrae **(Figure 13G-L)** and long bones **(Figure 14)** of wild type and *dtm* embryos.

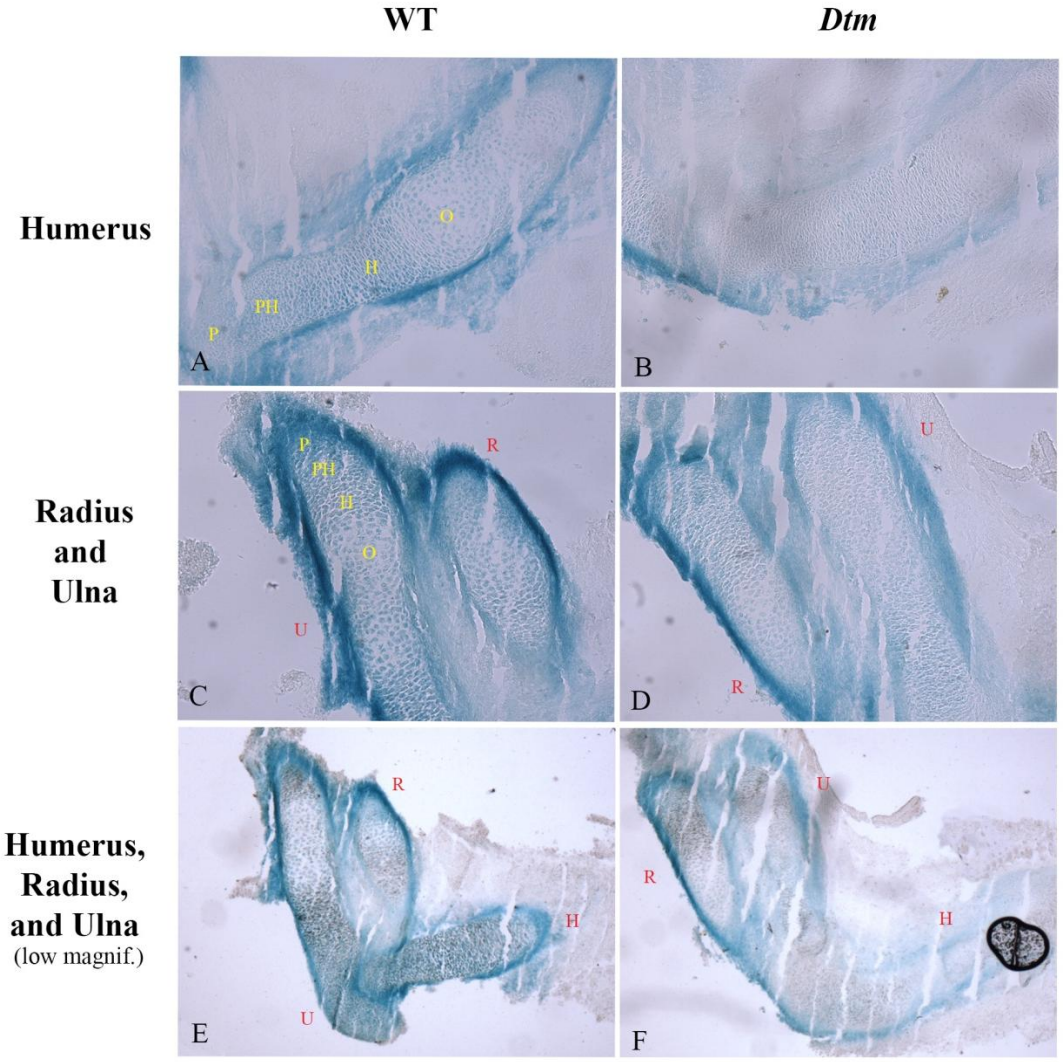

Figure 15 – *Dtm* embryos exhibit reduced *Ptch1* expression in the forelimb – X-gal-stained forelimb bone sections from mouse embryos expressing a *Ptch1-lacZ* reporter gene indicate lower *Ptch1* expression in *dtm* mutants **(B, D, F)** than in wild type **(A, C, E).** *Ptch1* expression is greatest in the perichondrium and in the proliferative and hypertrophic zones near the ends of the bones. Limb bones: Humerus (H), radius (R), ulna (U); Zones of developing bone: Proliferating (P), Prehypertrophic (PH), Hypertrophic (H), Ossifying (O)

Dtm mice exhibit rib and sternal vertebrae misalignment

In addition to a delay in endochondral ossification in the long bones and vertebrae, we noticed other interesting skeletal defects, including misalignment of the ribs and sternal vertebrae. In normal embryos, ribs are connected to the sternum in pairs and ossification of the sternum initiates in the inter-rib region **(Figure 16A, C)**. In contrast, *dtm* mice exhibited severe rib and sternal vertebrae misalignment **(Figure 16B, D)**. The misalignment was clearly observed as offset rib pairs and s-shaped ossified regions of the sternum, not as rectangular regions seen in wild type mice **(red stain in Figure 16A, C)**. In conjunction with the misalignment, *dtm* mice possessed an additional unpaired rib on one side at the most caudal point of attachment on the sternum **(Figure 16B, D)**.

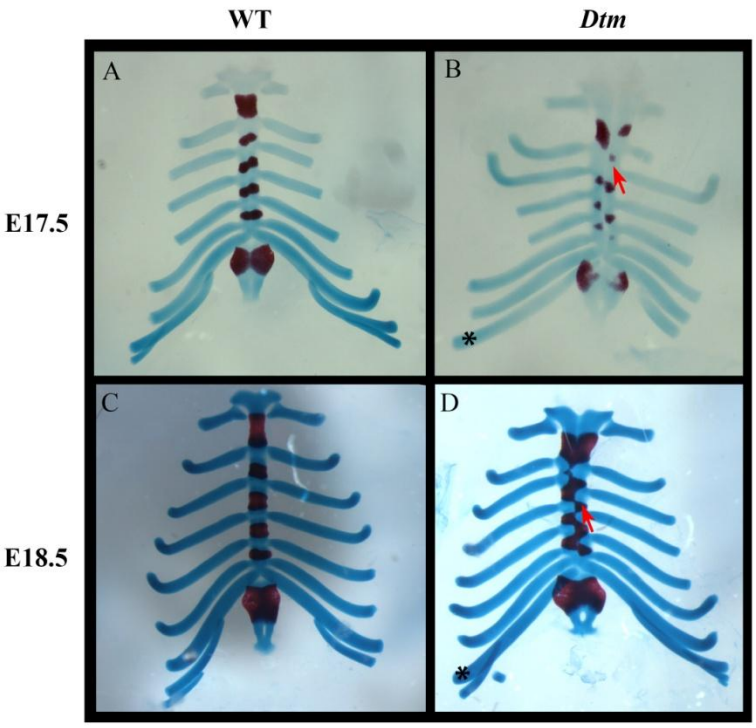

Figure 16 – *Dtm* mice exhibit rib and sternal vertebrae misalignment – Rib and sternal vertebrae misalignment in *dtm* mice **(B, D)** is indicated by the s-shaped sternal ossification (dark red staining, red arrow), uneven rib pairing, and the attachment of an extra rib (*) on the sternum, all of which are absent in wild type mice **(A, C)**, at E17.5 and E18.5.

HH SIGNALING AND CILIA-RELATED CHARACTERISTICS

Dtm mice exhibit mild polydactyly

Dtm mice are characterized by mild polydactyly, presenting with one extra digit (thumb) per limb **(Figure 17B, D)**. The size of the extra digit can vary among *dtm* individuals. Some mutants possess extra digits of normal length while others possess only small, knobby outgrowths on the normal thumb (not shown). The presence of polydactyly, combined with the known involvement of Shh signaling in limb patterning, suggests disruptions of Hh signaling.

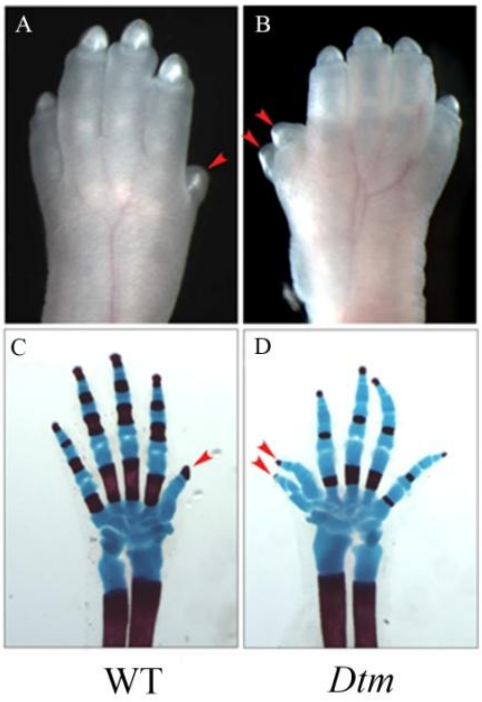

Figure 17 – *Dtm* mice exhibit polydactyly – Forelimb of E.18.5 wild type and *dtm* mice with thumbs indicated by red arrows **(A-B)** Whole mount **(C-D)** Bone (Alizarin Red) and cartilage (Alcian Blue) staining

Dtm embryos may exhibit developmental delays in neural tube patterning

To further evaluate the impact of the *dtm* mutation on Hh signaling, we examined the expression pattern of neural development markers regulated by the Shh gradient at E10.5. *Pax6* was expressed equally in wild type and mutant embryos, but the boundaries of *Nkx2.2*, *Foxa2*, and *Islet1* expression were less defined and expanded more dorsally in *dtm* individuals **(Figure 18A-H)**. An overlap of *Foxa2* and *Nkx2.2*-expressing cells was also seen in the mutant sample **(Figure 18E-F)**. These results suggest a potential developmental delay in the compaction and segregation of neural tube cells in *dtm* mutants. Further studies at a later stage would allow us to determine whether the differences in marker expression pattern persist.

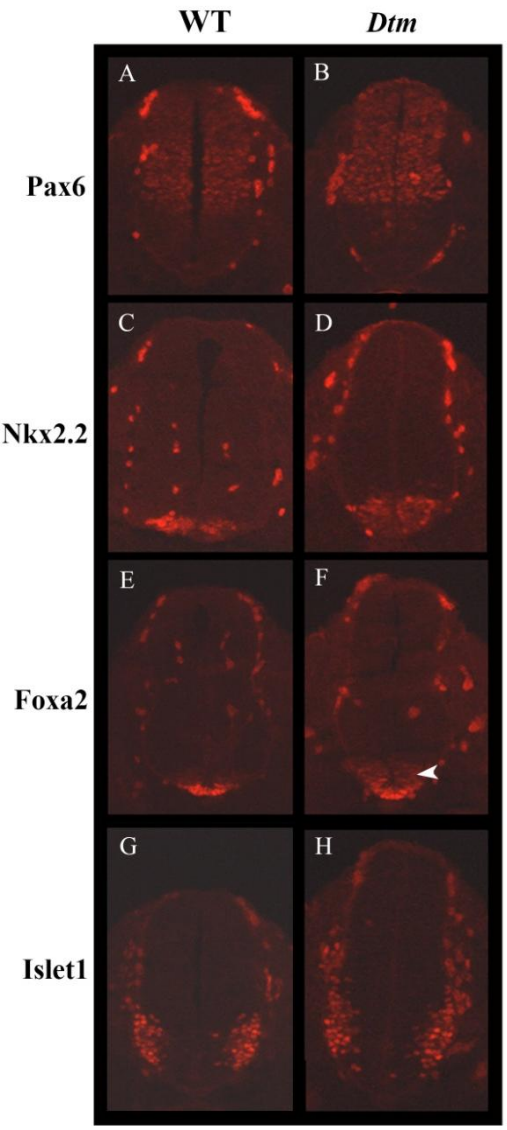

Figure 18 – Expression of neural markers suggest a possible neural patterning delay in *dtm* mutants – (A-B) No clear difference in *Pax6* expression between wild type and *dtm* embryos. **(C-D)** More dorsally expanded *Nkx2.2* expression in *dtm* embryos. **(E-F)** More dorsally expanded *Foxa2* expression and overlap of *Foxa2* and *Nkx2.2*-expressing cells (arrow) in *dtm* embryos. **(G-H)** More dorsally expanded *Islet1* expression in *dtm* embryos. Images from the forelimb region of E10.5 mutants.

Dtm mutants exhibit reduced ciliation

The skeletal and neural tube defects in *dtm* individuals are consistent with Hh-related defects, suggesting that Hh signaling may be affected by the *dtm* mutation. Our previous studies indicated that *Intu* is essential for cilia formation and that cilia is required for Hh signaling (Liu et

al., 2005; Zeng et al., 2010). Therefore, we tested the hypothesis that the *dtm* mutation disrupts cilia formation, which leads to compromised Hh signaling. Since primary cilia are important in kidney function and nervous system development, we examined the effects of the *dtm* mutation on ciliation in these tissues (Berbari et al., 2013; Briscoe and Ericson, 2001). We observed an average of 54.7% fewer cilia in kidney sections of PW6 *dtm* mice than in wild type sections of comparable cell density **(Figure 19A-B)**. The difference was highly significant (p=0.000002). While the number of cilia was not quantified for the ventral node, qualitative observation indicated shorter and fewer cilia in *dtm* mutants at E8.0 **(Figure 19C)**. These results suggest cilia formation is compromised in *dtm* mutants, which may underlie the aforementioned skeletal and neural tube defects.

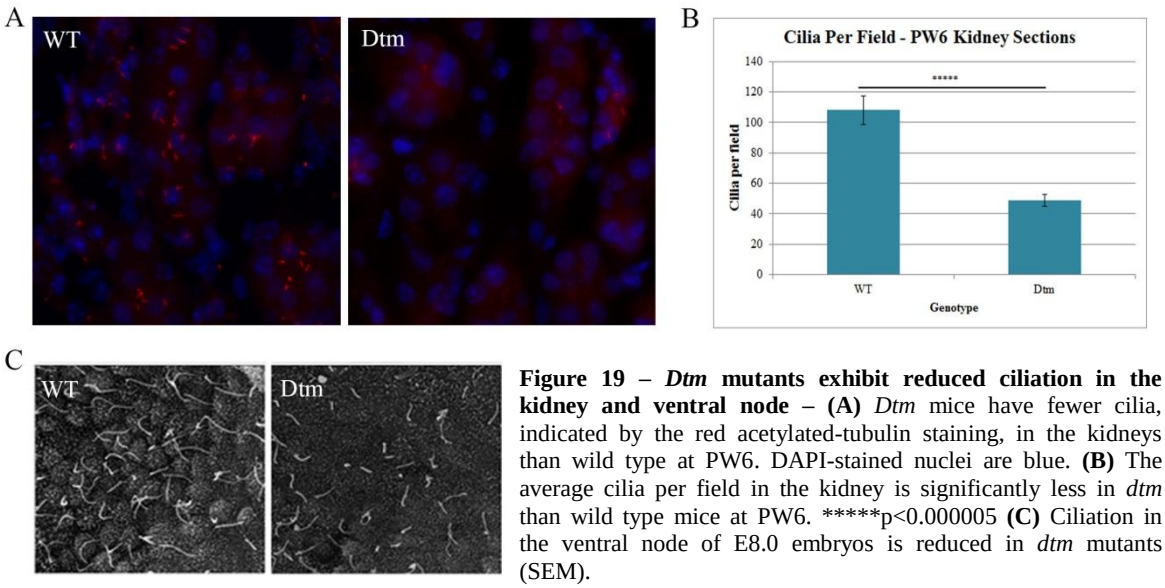

Figure 19 – *Dtm* mutants exhibit reduced ciliation in the kidney and ventral node – (A) *Dtm* mice have fewer cilia, indicated by the red acetylated-tubulin staining, in the kidneys than wild type at PW6. DAPI-stained nuclei are blue. **(B)** The average cilia per field in the kidney is significantly less in *dtm* than wild type mice at PW6. *****p<0.000005 **(C)** Ciliation in the ventral node of E8.0 embryos is reduced in *dtm* mutants (SEM).

Preliminary *in vitro* experiments suggest that the *dtm* mutation may have compromised the ability of the Intu protein to rescue ciliation in *Intu*$^{-/-}$ cells

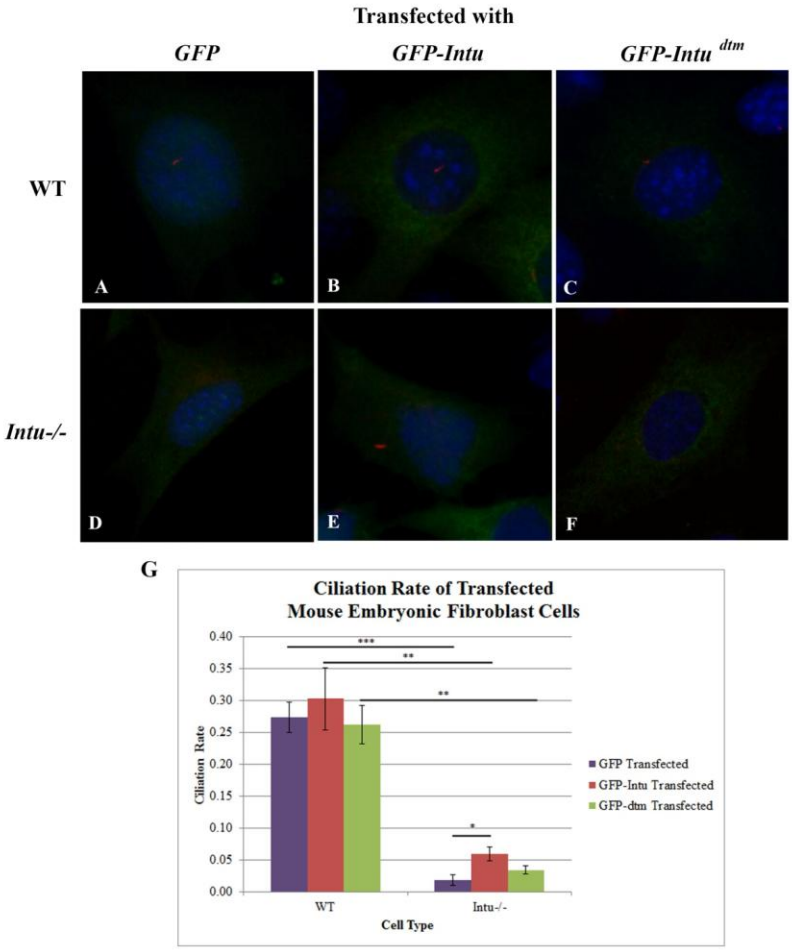

Figure 20 – Preliminary *in vitro* experiments suggest that the *dtm* mutation may have compromised the ability of the Intu protein to rescue ciliation in *Intu*$^{-/-}$ cells – (A-C) Wild type cells transfected with *GFP*, *GFP-Intu*, and *GFP-Intu*^{dtm} grew cilia (red, acetylated-tubulin [cilia]; blue, DAPI [nuclei]; green, GFP [transfected]). **(D-F)** *GFP* and *GFP-Intu*^{dtm} failed to rescue ciliation in *Intu*$^{-/-}$ cells. Interestingly, only a partial rescue was observed with *GFP-Intu* transfection. **(G)** Ciliogenesis was not fully rescued in *Intu*$^{-/-}$ cells, though a partial rescue was observed in the presence of *GFP-Intu*. *p<0.05, **p<0.005, ***p<0.0005

To further evaluate the impact of the *dtm* mutation on *Intu* function, we conducted *in vitro* cilia rescue studies with embryonic *Intu*$^{-/-}$ limb cells **(Figure 20)**. As previously reported, ciliation is almost completely disrupted in the *Intu* mutant cells **(Figure 19)**. *GFP-Intu* over-expression partially rescued the ciliation defects (p=0.01) **(Figure 20E, G)**. In contrast, GFP-Intu^{dtm} does not appear to rescue the ciliation in *Intu*$^{-/-}$ cells, suggesting that the mutation significantly disrupted the protein function (p=0.004) **(Figure 20F-G).** It is somewhat surprising that the ciliation rate in *Intu* mutant cells **(Figure 20D-G)** is still significantly lower than that in wild type cells **(Figure 20A-C, G)**, even in the presence of GFP-Intu (p=0.003), suggesting a rather inefficient rescue. More experiments are thus needed to improve the rescue efficiency.

DISCUSSION

Intu mediates Shh and Ihh signaling

The characteristics we observed in *dtm* mice – polydactyly **(Figure 17)**, reduced ossification in the vertebrae **(Figure 13G-L)**, digits **(Figure 13A-F)**, and forelimb bones **(Figure 14)**, reduced Ptch1 activity in the forelimb bones **(Figure 15)**, and altered expression of neural markers in the spinal cord **(Figure 18)** – suggest that the *dtm* mutation alters Hh signaling. This hypothesis is consistent with the results of our previous *in vivo* and *in vitro* studies of *Intu* null mutants (Zeng et al., 2010). These studies revealed that *Intu* mediates Hh signaling for limb patterning and central nervous system development, which are known roles of Shh signaling and characteristics that are also mildly affected in *dtm* mutants (Jacob and Briscoe, 2003; Laufer et al., 1994; Litingtung et al., 2002; Lopezmartinez et al., 1995; Riddle et al., 1993; Zeng et al., 2010).

In addition to Shh signaling, the skeletal defects and stunted growth in *dtm* mutants suggest that *Intu* also plays a role in Ihh signaling (Lai and Mitchell, 2005; Maeda et al., 2007; St-Jacques et al., 1999). Our previous studies showed that *Intu* null mutants exhibit disrupted proteolytic processing of Gli3, likely due to insufficient ciliation (Zeng et al., 2010). Given the reduced ciliation we observed in *Intu-/-* limb cells and the ventral node and kidney of *dtm* mice, a similar mechanism potentially underlies the observed Ihh-related phenotype **(Figure 19)**. Gli3 is an important part of the Ihh/PTHrP feedback mechanism for endochondral ossification **(Figure 6)** (Joeng and Long, 2009). Unbalanced levels of Gli3 repressor can disrupt the feedback loop and cause reduced chondrocyte proliferation and premature chondrocyte hypertrophy that leads to

decreased bone growth (Hellemans et al., 2003; Karp et al., 2000; Maeda et al., 2007; Razzaque et al., 2005; St-Jacques et al., 1999).

Intu-regulated ciliogenesis mediates Hh signaling

The characteristics of *dtm* individuals are partly reminiscent of some IFT and motor protein mutants, which further supports the notion that *Intu* mediates Hh signaling through the regulation of ciliogenesis. *Ift25* null mutants exhibit mild polydactyly and rib misalignment similar to that observed in *dtm* mice (Keady et al., 2012). The presence of neural tube patterning defects in E9.5 *Ift25* null mice that resolve by E10.5, including expanded *Pax6* expression, is also consistent with the normal *Pax6* expression in *dtm* mice at E10.5. It will be interesting to determine whether the expression of *Pax6,* as well as *Nkx2.2, Islet1,* and *Foxa2,* is transiently altered at E9.5 in *dtm* mutants. Although additional studies are needed to determine if Shh-related heart and palate structure defects found in *Ift25* null mutants are also present in *dtm* mice, it is unlikely that *dtm* mice have similarly severe defects. *Ift25* null mice survive to birth but die at P0 due to heart and respiratory defects. *Dtm* mice do not appear cyanotic at birth and have consistent survival once they survive past PW2. The similarity of some of the milder *dtm* and *Ift25* null characteristics suggests that normal *Ift25* activity may be reduced by the *dtm* mutation. Since *Ift25* is not required for ciliogenesis but is required for removing Smo and Ptch1 from the cilia and localizing Gli2 to the tip of the cilia, the *dtm* mutation also likely affects the activity of other ciliogenic genes (Keady et al., 2012).

Other candidates that may be affected in *dtm* mutants include *Ift80, Ift88,* and *Kif3a,* all of which are required for ciliogenesis and affect skeletal development (Huangfu et al., 2003; Yang and Wang, 2012). *Ift80,* expressed during early stages of osteoblast differentiation, promotes calcium and phosphate deposition (Yang and Wang, 2012). *In vitro* studies demonstrate that *Ift80* mutant cells exhibit reduced bony matrix deposition, likely due to disrupted Gli2

activation (Yang and Wang, 2012). This may explain, in part, the reduced ossification observed in *dtm* individuals. Ciliation is also reduced from 75-80% in wild type cells to 15-20% in *Ift80* mutant cells (Yang and Wang, 2012). A minority of mutant cells also possessed shortened cilia. The impact of *Ift80* mutation on ciliation is similar to the reduction but not absence of ciliation in *dtm* individuals. However, the long, narrow rib cage, short long bones, and short ribs of *Ift80* mutants are not seen in *dtm* individuals although both mutants present with polydactyly (Beales et al., 2007; Humke et al., 2010).

Cartilage-specific *Ift88* mutants exhibit disrupted chondrocyte organization, premature chondrocyte hypertrophy, and reduced ciliation within postnatal growth plates (Chang and Serra, 2013; Song et al., 2007). Decreased Ptch1 and Gli1 levels in the growth plates of cartilage-specific *Ift88* mutants are similarly observed in cartilage-specific *Ihh* mutants (Chang and Serra, 2013). These studies therefore support the hypothesis that the stunted postnatal growth of *dtm* mutants results from reduced Ihh signaling due to inadequate ciliogenesis. However, we have only examined embryonic growth plates **(Figure 15)**. Additional studies of Ptch1 and Gli activity and ciliation in the growth plates of postnatal *dtm* mice are needed for comparison.

In addition, defects in *Kif3a,* a Kinesin motor subunit, primarily cause postnatal skeletal defects similar to the *dtm* phenotype (Song et al., 2007). Cartilage-specific *Kif3a* mutants experience postnatal dwarfism, which is consistent with the small absolute difference in birth weight between wild type and *dtm* mice and the significantly reduced postnatal weight and size of *dtm* mice (Song et al., 2007). It is suspected that the stunted growth in cartilage-specific *Kif3a* mutants results from the premature termination of the chondrocyte proliferation and the premature initiation of chondrocyte hypertrophy due to the absence of cilia (Song et al., 2007). Since ciliation is reduced but not absent in *dtm* mice, the *dtm* mutation probably does not completely eliminate *Kif3a* function, if it is affected at all.

The similarity of the *dtm* phenotype to skeletal and ciliary abnormalities found in IFT and motor protein mutants therefore suggests that *Intu* regulates Hh signaling through the mediation of ciliogenesis.

Intu potentially affects alternative pathways for skeletal development

In addition to Ihh signaling, it is possible that the *dtm* mutation also affects skeletal development through other pathways. For example, an Ihh/FGF18 (fibroblastic growth factor)/FGFR3 (FGF receptor) feedback loop regulates chondrocyte proliferation and differentiation (Horton and Degnin, 2009). Ihh increases FGF18 secretion, which upregulates FGFR3 activity in the growth plate once chondrocyte proliferation and differentiation has reached sufficient levels. FGFR3 prevents bone lengthening by inhibiting chondrocyte proliferation, differentiation, and matrix deposition. Ihh activity is subsequently reduced through negative feedback. Therefore, it is possible that the reduced skeleton size of *dtm* individuals results from disruption of this feedback mechanism, which has been implicated in achondroplasia dwarfism (Horton et al., 2007).

The relationship between *IGF1* (insulin-like growth factor)/*IGFR1* (IGF receptor) and Ihh has also been studied in the context of skeletal development (Long et al., 2006; Wang et al., 1995). *IGFR1*$^{-/-}$ mutants generally die immediately after birth from respiratory failure and exhibit reduced birth weight (60% of wild type) and body size (45% of wild type) (Liu et al., 1993). They also experience delayed ossification (Liu et al., 1993). *IGFR1;Ihh* double knockout mice are characterized by lower birth weights and more severe dwarfism than either single mutant, indicating that *IGFR1* and Ihh regulate bone growth independently of one another (Long et al., 2006). Although the *dtm* mortality and weight and size deficit is much milder than that of these knockout mice, it is possible that the *dtm* mutation alters, but does not eliminate *IGF* function, in addition to modifying Ihh activity.

Other explanations unrelated to Hh signaling or cilia for the smaller size of *dtm* individuals are also possible. Given that the difference in wild type and *dtm* body size is greatest postnatally, nutritional issues shortly after birth may account for the stunted growth. Maternal deprivation, lack of interaction with or separation from the mother, can lead to nutrient deprivation (Ding et al., 2010). Heat deprivation as a consequence of maternal deprivation can exacerbate the nutrient and growth deficits (Ding et al., 2010). Such circumstances can cause neonatal stress, which has been shown to make mice more vulnerable to weight loss, anorexia, and reduced appetite as adults (Avitsur and Sheridan, 2009). Evaluation of newborn behavior will help to prove or eliminate this possibility.

Intu does not play an essential role in PCP

Since *Intu* is a PCP effector gene, it is also possible that the stunted growth of *dtm* mutants may be attributable to altered PCP signaling, as PCP signaling has been implicated in chondrocyte alignment (Li and Dudley, 2009). However, this is unlikely because minimal PCP-related defects were observed in *Intu* null mutants, suggesting that *Intu* does not play an essential role in PCP (Zeng et al., 2010).

Additional experimentation

Our preliminary studies of the *dtm* mutant phenotype have yielded some exciting results. However, more experiments are needed to corroborate and expand on our results. For the body weight study, only three *dtm* mice were available at later stages due to the loss of some *dtm* mutants (compared to n_{dtm}=13 at P0). This likely accounts for the absence of statistical significance at PW5 and PW6 in spite of the clear divergence between wild type and mutant body weights. In the bone ossification and bone length studies, only one to three *dtm* individuals were available for each time point. Additional samples are needed to determine whether the observed

differences in ossification reflect true differences, natural variation, or artifacts of incongruent embryo staging and/or depth of field variations of images from which measurements were taken. In addition, these measurements should be taken at postnatal stages when the body weight difference between wild type and *dtm* mutants is significant.

Modifications to the experimental system in the *in vitro* cilia rescue studies are also needed to improve transfection efficiency and optimize cilia induction. Optimizing the density of cells, length of starvation period, length of the post-transfection incubation, and amount of DNA used may produce more consistent data. Examining the ciliation in chondrocytes would also be helpful for understanding the local cellular activity in developing bone.

To gain a more thorough understanding of the temporal distribution of *dtm* mutation effects, repeating ossification, spinal cord immunohistochemistry, and ciliation studies at additional time points is necessary. The differences in ossification in the digits of wild type and *dtm* mice persisted throughout E16.5-E18.5, while differences in the vertebrae resolved. Evaluating ossification when it typically begins at E13.5 through postnatal ages would allow us to determine whether delays or permanent reductions in ossification exist in mutant individuals. Such experiments, in addition to studying Ptch1 activity at similar stages, would also clarify the timing of those differences. In addition, evaluating the expression of neural markers in the spinal cord at time points earlier and later than E10.5 would clarify the nature of the differences in neural cell differentiation. These studies would reveal whether a delay exists, in which case the differences would resolve, or the differences reflect natural variation. Investigating the ciliation rate in the kidney at time points younger than PW6 would achieve similar goals. Understanding the effect of the *dtm* mutation on ciliation and Hh signaling can help to elucidate the etiology of the *dtm* phenotype. In all of these experiments, postnatal time points are important since the diverging body weights suggest that the mutation has persisting postnatal effects.

Future direction

In the present study, we primarily examined the bones that undergo endochondral ossification. Expanding our studies to other bones, including ones that undergo intramembranous ossification, would contribute to a more complete understanding of the role of *Intu*. We could also explore the morphology and size of organs, such as the brain, heart, and lungs, in *dtm* mutants. This would allow us to compare the *dtm* characteristics to those of other published IFT, PCP, and Hh-related mutants in order to better identify the proteins whose activity is disrupted by the *dtm* mutation.

Although the characteristics of *dtm* mice suggest the involvement of Shh and Ihh signaling, we have yet to explore the involvement of Dhh signaling. Evaluating fertility through breeding of *dtm* individuals is one possible avenue for beginning this investigation.

After gaining an understanding of the developmental nature of the *dtm* phenotype, it would be interesting to explore which parts of the *Intu* gene are responsible for function. This can be achieved through *in vitro* studies looking at the ciliogenic and osteogenic capabilities of cells transfected with variants of *Intu*. Findings from such studies could be used to investigate the evolutionary conservation of *Intu* across species and may provide additional insight on the function and behavior of PCP effector genes.

Conclusion

Our studies of the *dtm* mutant, though preliminary, suggest that the PCP effector gene *Intu* promotes ciliogenesis, skeletal patterning and growth, and neural tube patterning in mammalian embryonic development. The actions of *Intu* involve Hh signaling, including Shh and Ihh. Understanding the genetic and molecular basis of ciliogenesis and skeletal defects has the potential to advance our knowledge of the pathology of ciliopathies in humans. These insights may one day translate to viable, more effective treatments for these congenital disorders.

MATERIALS AND METHODS

Generation of Intu$^{dtm/dtm}$; *Ptch1-lacZ* transgenic embryos

Ptch1-lacZ transgenic mice were genotyped based on the methods described in Goodrich et al., 1997.

Intu$^{dtm/+}$ females were mated with *Intu*$^{dtm/+}$*; Ptch1-lacZ* males to produce homozygous Intu$^{dtm/dtm}$*; Ptch1-lacZ* embryos. Genomic DNA was prepared by incubating tail snips overnight in 100ul lysis buffer (50mM Tris·HCl, pH8.8, 1mM EDTA and 0.5% Tween 20) with proteinase K (100µg/mL) at 55ºC. Embryos were genotyped for *lacZ* by polymerase chain reaction (PCR) on genomic DNA using primers CCGAACCATCCGCTGTGGTAC and CATCCACGCGCGCGTACATC. The electrophoresis of the PCR products was performed using ethidium bromide-stained agarose gels.

X-gal staining of *Ptch1-lacZ* transgenic embryos

Embryos were dissected and fixed in 4% paraformaldehyde (PFA) for 1-3 hours at 4ºC. Subsequently, embryos were washed three times for 15 minutes per wash using wash buffer (0.1 M phosphate buffer, 2 mM $MgCl_2$ and 0.02% Nonidet P-40) and stained overnight at 37ºC in X-gal solution (in wash buffer: 5 mM potassium ferrocyanide [$K_3Fe(CN)_6$], 5 mM potassium ferricyanide [$K_4Fe(CN)_6.3H_2O$], 1 mg/mL X-gal [5-Bromo-4-chloro-3-indolyl β-D-galactopyranoside, Sigma] and 0.01% sodium deoxycholate for improved penetration). After

staining, the embryos were washed using wash buffer three times for five minutes per wash and stored in 4% PFA at 4ºC until further processing and imaging.

For sectioning, fixed X-gal-stained embryos were washed three times in cold phosphate buffered saline (PBS) for 15 minutes per wash. The tissue was then submerged in 30% sucrose in PBS and incubated in Tissue Tek OCT compound before freezing. The tissue was sectioned at10µm and allowed to air dry for one hour. Sections were stored at -80ºC until mounted and imaged on the Nikon E600 microscope at 4x and 10x magnification.

Bone and cartilage staining

Embryos were soaked in water for 24 hours prior to skin removal and evisceration. Embryos were then fixed in 95% ethanol for three days followed by staining in cartilage-specific Alcian Blue solution for 24 hours (for 50mL solution: 10mL glacial acetic acid, 40mL 95% ethanol, 7.5mg Alcian Blue 8GX, Fluka). Subsequently, embryos were rinsed with 95% ethanol and stained in fresh Alcian Blue for an additional 24 hours. Embryos were then stained in bone-specific Alizarin Red (Harleco) solution (50mg Alizarin Red per liter of 2% potassium hydroxide [KOH]) for three hours, rinsed in 95% ethanol, and stained in fresh Alizarin Red overnight.

Samples were cleared in 1% KOH for a few days and then transferred from 20 to 40, 60, and 80% glycerol solutions in 1% KOH over a few weeks to remove excess dye.

All whole mount embryo images were taken on the Zeiss KD2500 microscope. Whole embryo images were taken with 16.5x magnification (E11.5) and 8x magnification (E16.5-18.5). Limb images were taken with10x magnification (E16.5-18.5) and sternum images with 15x magnification.

Bone measurements were taken manually from images and reflect the maximum lengths. The ossified fraction of a bone was determined as shown in **Figure 21**. Measurements were standardized to account for variation in image magnification and animal body size.

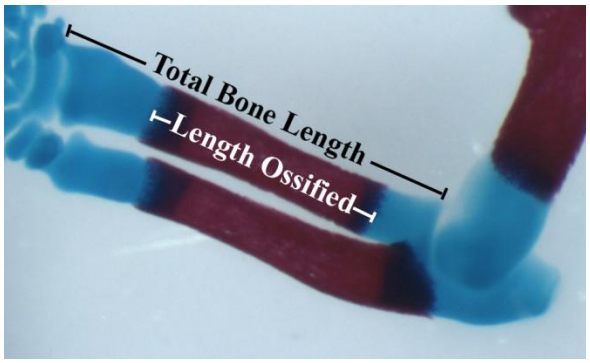

Figure 21 – Calculation of the ossified fraction of long bones

Fraction of bone ossified = $\frac{length\ ossified}{total\ bone\ length}$

Lengths are the measurements between the two furthest points on a given bone.

Immunohistochemistry

Kidney and spinal cord tissues were fixed in 4% PFA for two hours on ice and prepared and sectioned as described above (see "X-gal staining of *Ptch1-lacZ* transgenic embryos").

Sections stored at -80ºC were dried for one hour at room temperature and then incubated in blocking buffer (1% normal goat serum [NGS], 0.1% Triton X-100 in PBS) for one hour. Sections were incubated overnight in primary antibody at 4ºC. The primary antibody used for the kidney sections was rabbit α-mouse ARL13B (1:1000 dilution, Tamara Caspary). The primary mouse antibodies used for spinal cord sections included Nkx2.2 (1:40), Pax6 (1:500), Islet1 (1:1000), and Foxa2 (1:40), all from the Developmental Studies Hybridoma Bank. Slides were washed three times for 10 minutes per wash in blocking buffer and then incubated in secondary antibody for one hour at room temperature. The secondary antibody used for the kidney sections was Cy3-conjugated goat α-rabbit (1:250, Jackson ImmunoResearch). The secondary antibody used for the spinal cord sections was Cy3-conjugated goat α-mouse IgG (1:250, Jackson ImmunoResearch). All antibodies were diluted in blocking buffer. Slides were washed three times for 10 minutes per wash and mounted with Vectashield mounting medium. Slides were stored at 4ºC until imaged.

The tissue sections were visualized with the Nikon E600 microscope. Kidney sections were imaged at 40x magnification. Spinal cord sections were imaged at 10x magnification.

Generation of the *GFP-Intu*^{dtm} fusion protein construct

The *GFP-Intu*^{dtm} fusion protein construct was generated by introducing the *dtm* point mutation into the previously generated *GFP-Intu* construct (Zeng et al., 2010). The primers used were ACACCCCCACCCATGAAGAG and TGAAGATGCCTTGCACTGTTTCC. The PCR product was purified with the QIAquick PCR Purification Kit (Qiagen), self-ligated, and was used to transform competent cells. The *dtm* point mutation was verified by digestion with HindIII (2.3kb and 5kb products) and sequencing with GFP primers ATGGTCCTGCTGGAGTTCGT and GGGAGGTGTGGGAGGTTTT and *Intu* primers GCTATGAAGAGCGGTCAGGT and ATGTTGGAGAGGCTGCTGTT.

Cell culture

Wild type and *Intu*$^{-/-}$ mouse limb fibroblasts (E12.5, immortalized with SV40 large T antigen) (Zeng et al., 2010)) were maintained at 37ºC and 5% CO_2 in media (Dulbecco's modified eagle's medium [DMEM], 10% fetal bovine serum [FBS], 2 mM GlutaMAX, penicillin [100U/mL]-streptomycin [100µg/mL]). Cells were allowed to proliferate to 90-95% confluence on plates coated with 0.1% gelatin before passing.

Immunocytochemistry

Confluent cells were passed onto 0.1% gelatin-coated coverslips in media without antibiotics (DMEM, 10% FBS, 2mM GlutaMAX) the day prior to transfection. The cell dilution was adjusted so that the cells would reach ~50% confluence within 24 hours. DNA (*GFP*, *GFP-Intu*, or *GFP-Intu*^{dtm}; 0.8µg/50µL opti-MEM/coverslip) and Lipofectamine 2000 (Invitrogen, 2µL/50µL opti-MEM/coverslip) were combined and incubated at room temperature for 20 minutes. Cells were then transfected with 100µL of the solution per coverslip in a 24-well plate. The transfected cells were incubated in media without antibiotics for 10-12 hours and then

starved for 24 hours (DMEM, 0.5% FBS, 2mM GlutaMAX, penicillin [100U/mL]-streptomycin [100µg/mL]) to allow cilia to grow.

Cells were harvested and rinsed with warm PBS prior to fixation in 4% PFA for 10 minutes at room temperature. Cells were then rinsed twice with PBST (PBS, 0.1% Triton X-100) and blocked with a solution of PBST+10% NGS for 10 minutes. Subsequently, cells were incubated in primary antibody overnight at 4ºC (α-acetylated tubulin, 1:1000 dilution, Sigma; GFP, 1:500, Invitrogen). Cells were then rinsed three times with PBST and incubated in secondary antibody for two hours at room temperature (Cy3-conjugated goat α-mouse, 1:500, Jackson ImmunoResearch; AF-488 goat α-rabbit, 1:500). All antibodies were diluted in a solution of PBS+10% NGS. Following three washes with PBST and one wash with water, the coverslips were mounted onto glass slides with Vectashield mounting medium with DAPI.

The slides were stored at 4ºC and visualized under a Nikon E600 microscope and imaged at 60x magnification.

Statistical analyses

Data was analyzed using the Microsoft Excel function for unpaired, two-tailed T-tests.

BIBLIOGRAPHY

Aguero, T.H., Fernandez, J.P., Lopez, G.A.V., Tribulo, C., Aybar, M.J., 2012. Indian hedgehog signaling is required for proper formation, maintenance and migration of Xenopus neural crest. Developmental Biology 364, 99-113.

Ahlgren, S.C., Bronner-Fraser, M., 1999. Inhibition of Sonic hedgehog signaling in vivo results in craniofacial neural crest cell death. Current Biology 9, 1304-1314.

Arthur, H.M., Bamforth, S.D., 2011. TGF beta Signaling and Congenital Heart Disease: Insights from Mouse Studies. Birth Defects Res. Part A-Clin. Mol. Teratol. 91, 423-434.

Astorga, J., Carlsson, P., 2007. Hedgehog induction of murine vasculogenesis is mediated by Foxf1 and Bmp4. Development 134, 3753-3761.

Avitsur, R., Sheridan, J.F., 2009. Neonatal stress modulates sickness behavior. Brain Behav. Immun. 23, 977-985.

Baker, K., Beales, P.L., 2009. Making sense of cilia in disease: The human ciliopathies. American Journal of Medical Genetics Part C: Seminars in Medical Genetics 151C, 281-295.

Beales, P.L., Bland, E., Tobin, J.L., Bacchelli, C., Tuysuz, B., Hill, J., Rix, S., Pearson, C.G., Kai, M., Hartley, J., Johnson, C., Irving, M., Elcioglu, N., Winey, M., Tada, M., Scambler, P.J., 2007. IFT80, which encodes a conserved intraflagellar transport protein, is mutated in Jeune asphyxiating thoracic dystrophy. Nature Genetics 39, 727-729.

Berbari, N.F., Sharma, N., Malarkey, E.B., Pieczynski, J.N., Boddu, R., Gaertig, J., Guay-Woodford, L., Yoder, B.K., 2013. Microtubule modifications and stability are altered by cilia perturbation and in cystic kidney disease. Cytoskeleton 70, 24-31.

Bitgood, M.J., Shen, L.Y., McMahon, A.P., 1996. Sertoli cell signaling by Desert hedgehog regulates the male germline. Current Biology 6, 298-304.

Bowers, M., Eng, L., Lao, Z., Turnbull, R.K., Bao, X., Riedel, E., Mackem, S., Joyner, A.L., 2012. Limb anterior–posterior polarity integrates activator and repressor functions of GLI2 as well as GLI3. Developmental Biology 370, 110-124.

Briscoe, J., Ericson, J., 2001. Specification of neuronal fates in the ventral neural tube. Current Opinion in Neurobiology 11, 43-49.

Brodeur, G.M., Seeger, R.C., Schwab, M., Varmus, H.E., Bishop, J.M., 1984. Amplification of N-myc in untreated human neuroblastomas correlates with advanced disease stage. Science 224, 1121-1124.

Chang, C.-F., Serra, R., 2013. Ift88 regulates Hedgehog signaling, Sfrp5 expression, and beta-catenin activity in post-natal growth plate. Journal of Orthopaedic Research 31, 350-356.

Chiang, C., Ying, L.T.T., Lee, E., Young, K.E., Corden, J.L., Westphal, H., Beachy, P.A., 1996. Cyclopia and defective axial patterning in mice lacking Sonic hedgehog gene function. Nature 383, 407-413.

Clark, A.M., Garland, K.K., Russell, L.D., 2000. Desert hedgehog (Dhh) gene is required in the mouse testis for formation of adult-type Leydig cells and normal development of peritubular cells and seminiferous tubules. Biol. Reprod. 63, 1825-1838.

Collier, S., Lee, H., Burgess, R., Adler, P., 2005. The WD40 repeat protein fritz links cytoskeletal planar polarity to frizzled subcellular localization in the Drosophila epidermis. Genetics 169, 2035-2045.

Corbin, J.G., Rutlin, M., Gaiano, N., Fishell, G., 2003. Combinatorial function of the homeodomain proteins Nkx2.1 and Gsh2 in ventral telencephalic patterning. Development 130, 4895-4906.

Corbit, K.C., Aanstad, P., Singla, V., Norman, A.R., Stainier, D.Y.R., Reiter, J.F., 2005. Vertebrate Smoothened functions at the primary cilium. Nature 437, 1018-1021.

Corbit, K.C., Shyer, A.E., Dowdle, W.E., Gaulden, J., Singla, V., Reiter, J.F., 2008. Kif3a constrains beta-catenin-dependent Wnt signalling through dual ciliary and non-ciliary mechanisms. Nature Cell Biology 10, 70-U54.

Cridland, S.O., Keys, J.P., Papathanasiou, P., Perkins, A.C., 2009. Indian hedgehog supports definitive erythropoiesis. Blood Cells Mol. Dis. 43, 149-155.

Dang, C.V., 2012. MYC on the Path to Cancer. Cell 149, 22-35.

Ding, F., Li, H.H., Li, J., Myers, R.M., Francke, U., 2010. Neonatal Maternal Deprivation Response and Developmental Changes in Gene Expression Revealed by Hypothalamic Gene Expression Profiling in Mice. PLoS One 5.

Ding, Q., Fukami, S.I., Meng, X., Nishizaki, Y., Zhang, X., Sasaki, H., Dlugosz, A., Nakafuku, M., Hui, C.C., 1999. Mouse Suppressor of fused is a negative regulator of Sonic hedgehog signaling and alters the subcellular distribution of Gli1. Current Biology 9, 1119-1122.

Drossopoulou, G., Lewis, K.E., Sanz-Ezguerro, J.J., Nikbaklt, N., McMahon, A.P., Hofman, C., Tickle, C., 2000. A model for anteriorposterior patterning of the vertebrate limb based on sequential long-and short-range Shh signalling and BMP signalling. Development 127, 1337-1348.

Duman-Scheel, M., Weng, L., Xin, S.J., Du, W., 2002. Hedgehog regulates cell growth and proliferation by inducing cyclin D and cyclin E. Nature 417, 299-304.

Dyer, M.A., Farrington, S.M., Mohn, D., Munday, J.R., Baron, M.H., 2001. Indian hedgehog activates hematopoiesis and vasculogenesis and can respecify prospective neurectodermal cell fate in the mouse embryo. Development 128, 1717-1730.

Eaton, S., Julicher, F., 2011. Cell flow and tissue polarity patterns. Curr. Opin. Genet. Dev. 21, 747-752.

Eggenschwiler, J.T., Bulgakov, O.V., Qin, J., Li, T.S., Anderson, K.V., 2006. Mouse Rab23 regulates Hedgehog signaling from Smoothened to Gli proteins. Developmental Biology 290, 1-12.

Eggenschwiler, J.T., Espinoza, E., Anderson, K.V., 2001. Rab23 is an essential negative regulator of the mouse Sonic hedgehog signalling pathway. Nature 412, 194-198.

Evans, T.M., Ferguson, C., Wainwright, B.J., Parton, R.G., Wicking, C., 2003. Rab23, a negative regulator of hedgehog signaling, localizes to the plasma membrane and the endocytic pathway. Traffic 4, 869-884.

Garson, J.A., Pemberton, L.F., Sheppard, P.W., Varndell, I.M., Coakham, H.B., Kemshead, J.T., 1989. N-myc gene-expression and oncoprotein characterization in medulloblastoma. British Journal of Cancer 59, 889-894.

Gerhardt, H., Golding, M., Fruttiger, M., Ruhrberg, C., Lundkvist, A., Abramsson, A., Jeltsch, M., Mitchell, C., Alitalo, K., Shima, D., Betsholtz, C., 2003. VEGF guides angiogenic sprouting utilizing endothelial tip cell filopodia. Journal of Cell Biology 161, 1163-1177.

Gilbert, S.F., 2006. Developmental Biology, 8 ed. Sinauer Associates, Sunderland, MA.

Gilbert, S.F., 2010. Developmental Biology, 9 ed. Sinauer Associates, Sunderland, MA.

Goetz, S.C., Anderson, K.V., 2010. The primary cilium: a signalling centre during vertebrate development. Nature Reviews Genetics 11, 331-344.

Goodrich, L.V., Milenkovic, L., Higgins, K.M., Scott, M.P., 1997. Altered neural cell fates and medulloblastoma in mouse patched mutants. Science 277, 1109-1113.

Hahn, H., Wicking, C., Zaphiropoulos, P.G., Gailani, M.R., Shanley, S., Chidambaram, A., Vorechovsky, I., Holmberg, E., Unden, A.B., Gillies, S., Negus, K., Smyth, I., Pressman, C., Leffell, D.J., Gerrard, B., Goldstein, A.M., Dean, M., Toftgard, R., ChenevixTrench, G., Wainwright, B., Bale, A.E., 1996. Mutations of the human homolog of Drosophila patched in the nevoid basal cell carcinoma syndrome. Cell 85, 841-851.

Harfe, B.D., Scherz, P.J., Nissim, S., Tian, F., McMahon, A.P., Tabin, C.J., 2004. Evidence for an expansion-based temporal Shh gradient in specifying vertebrate digit identities. Cell 118, 517-528.

Harland, R.M., 1994. The transforming growth factor beta family and induction of the vertebrate mesoderm - bone morphogenic proteins are ventral inducers. Proceedings of the National Academy of Sciences of the United States of America 91, 10243-10246.

Haycraft, C.J., Banizs, B., Aydin-Son, Y., Zhang, Q.H., Michaud, E.J., Yoder, B.K., 2005. Gli2 and Gli3 localize to cilia and require the intra-flagellar transport protein polaris for processing and function. Plos Genetics 1, 480-488.

Hellemans, J., Coucke, P.J., Giedion, A., De Paepe, A., Kramer, P., Beemer, F., Mortier, G.R., 2003. Homozygous mutations in IHH cause acrocapitofemoral dysplasia, an autosomal recessive disorder with cone- shaped epiphyses in hands and hips. American Journal of Human Genetics 72, 1040-1046.

Heydeck, W., Liu, A.M., 2011. PCP Effector Proteins Inturned and Fuzzy Play Nonredundant Roles in the Patterning but Not Convergent Extension of Mammalian Neural Tube. Dev. Dyn. 240, 1938-1948.

Hojo, H., Ohba, S., Yano, F., Saito, T., Ikeda, T., Nakajima, K., Komiyama, Y., Nakagata, N., Suzuki, K., Takato, T., Kawaguchi, H., Chung, U., 2012. Gli1 Protein Participates in Hedgehog-mediated Specification of Osteoblast Lineage during Endochondral Ossification. J. Biol. Chem. 287, 17860-17869.

Horton, W.A., Degnin, C.R., 2009. FGFs in endochondral skeletal development. Trends in Endocrinology & Metabolism 20, 341-348.

Horton, W.A., Hall, J.G., Hecht, J.T., 2007. Achondroplasia. Lancet 370, 162-172.

Huangfu, D., Anderson, K.V., 2005. Cilia and Hedgehog responsiveness in the mouse. Proceedings of the National Academy of Sciences of the United States of America 102, 11325-11330.

Huangfu, D.W., Liu, A.M., Rakeman, A.S., Murcia, N.S., Niswander, L., Anderson, K.V., 2003. Hedgehog signalling in the mouse requires intraflagellar transport proteins. Nature 426, 83-87.

Humke, E.W., Dorn, K.V., Milenkovic, L., Scott, M.P., Rohatgi, R., 2010. The output of Hedgehog signaling is controlled by the dynamic association between Suppressor of Fused and the Gli proteins. Genes & Development 24, 670-682.

Ignelzi, M.A., Wang, W., Young, A.T., 2003. Fibroblast growth factors lead to increased Msx2 expression and fusion in calvarial sutures. J. Bone Miner. Res. 18, 751-759.

Inada, M., Yasui, T., Nomura, S., Miyake, S., Deguchi, K., Himeno, M., Sato, M., Yamagiwa, H., Kimura, T., Yasui, N., Ochi, T., Endo, N., Kitamura, Y., Kishimoto, T., Komori, T., 1999. Maturational disturbance of chondrocytes in Cbfa1-deficient mice. Dev. Dyn. 214, 279-290.

Jacob, J., Briscoe, J., 2003. Gli proteins and the control of spinal-cord patterning. Embo Reports 4, 761-765.

Jensen, A.M., Wallace, V.A., 1997. Expression of Sonic hedgehog and its putative role as a precursor cell mitogen in the developing mouse retina. Development 124, 363-371.

Joeng, K.S., Long, F.X., 2009. The Gli2 transcriptional activator is a crucial effector for Ihh signaling in osteoblast development and cartilage vascularization. Development 136, 4177-4185.

Johnson, R.L., Rothman, A.L., Xie, J.W., Goodrich, L.V., Bare, J.W., Bonifas, J.M., Quinn, A.G., Myers, R.M., Cox, D.R., Epstein, E.H., Scott, M.P., 1996. Human homolog of patched, a candidate gene for the basal cell nevus syndrome. Science 272, 1668-1671.

Jones, C., Chen, P., 2007. Planar cell polarity signaling in vertebrates. BioEssays 29, 120-132.

Jones, C., Roper, V.C., Foucher, I., Qian, D., Banizs, B., Petit, C., Yoder, B.K., Chen, P., 2008. Ciliary proteins link basal body polarization to planar cell polarity regulation. Nature Genetics 40, 69-77.

Karp, S.J., Schipani, E., St-Jacques, B., Hunzelman, J., Kronenberg, H., McMahon, A.P., 2000. Indian hedgehog coordinates endochondral bone growth and morphogenesis via Parathyroid Hormone related-Protein-dependent and -independent pathways. Development 127, 543-548.

Kawakami, Y., Ishikawa, T., Shimabara, M., Tanda, N., EnomotoIwamoto, M., Iwamoto, M., Kuwana, T., Ueki, A., Noji, S., Nohno, T., 1996. BMP signaling during bone pattern determination in the developing limb. Development 122, 3557-3566.

Keady, Brian T., Samtani, R., Tobita, K., Tsuchya, M., San Agustin, Jovenal T., Follit, John A., Jonassen, Julie A., Subramanian, R., Lo, Cecilia W., Pazour, Gregory J., 2012. IFT25 Links the Signal-Dependent Movement of Hedgehog Components to Intraflagellar Transport. Developmental Cell 22, 940-951.

Keller, R., 2002. Shaping the vertebrate body plan by polarized embryonic cell movements. Science 298, 1950-1954.

Kenney, A.M., Cole, M.D., Rowitch, D.H., 2003. Nmyc upregulation by sonic hedgehog signaling promotes proliferation in developing cerebellar granule neuron precursors. Development 130, 15-28.

Komada, M., 2012. Sonic hedgehog signaling coordinates the proliferation and differentiation of neural stem/progenitor cells by regulating cell cycle kinetics during development of the neocortex. Congenit. Anom. 52, 72-77.

Komori, T., 2011. Signaling Networks in RUNX2-Dependent Bone Development. J. Cell. Biochem. 112, 750-755.

Kucerova, R., Dora, N., Mort, R.L., Wallace, K., Leiper, L.J., Lowes, C., Neves, C., Walczysko, P., Bruce, F., Fowler, P.A., Rajnicek, A.M., McCaig, C.D., Zhao, M., West, J.D., Collinson, J.M., 2012. Interaction between hedgehog signalling and PAX6 dosage mediates maintenance and regeneration of the corneal epithelium. Mol. Vis. 18, 139-150.

Kuspert, M., Weider, M., Muller, J., Hermans-Borgmeyer, I., Meijer, D., Wegner, M., 2012. Desert Hedgehog Links Transcription Factor Sox10 to Perineurial Development. J. Neurosci. 32, 5472-5480.

Lai, L.P., Mitchell, J., 2005. Indian hedgehog: Its roles and regulation in endochondral bone development. J. Cell. Biochem. 96, 1163-1173.

Lau, C.I., Outram, S.V., Saldana, J.I., Furmanski, A.L., Dessens, J.T., Crompton, T., 2012. Regulation of murine normal and stress-induced erythropoiesis by Desert Hedgehog. Blood 119, 4741-4751.

Laufer, E., Nelson, C.E., Johnson, R.L., Morgan, B.A., Tabin, C., 1994. Sonic Hedgehog and FGF-4 act through a signaling cascade and feedback loop to integrate growth and patterning of the developing limb bud. Cell 79, 993-1003.

Lee, W.H., Murphree, A.L., Benedict, W.F., 1984. Expression and amplification of the N-myc gene in primary retinoblastoma. Nature 309, 458-460.

Li, Y., Dudley, A.T., 2009. Noncanonical frizzled signaling regulates cell polarity of growth plate chondrocytes. Development 136, 1083-1092.

Litingtung, Y., Dahn, R.D., Li, Y.N., Fallon, J.F., Chiang, C., 2002. Shh and Gli3 are dispensable for limb skeleton formation but regulate digit number and identity. Nature 418, 979-983.

Liu, A.M., unpublished.

Liu, A.M., Wang, B.L., Niswander, L.A., 2005. Mouse intraflagellar transport proteins regulate both the activator and repressor functions of Gli transcription factors. Development 132, 3103-3111.

Liu, J.P., Baker, J., Perkins, A.S., Robertson, E.J., Efstratiadis, A., 1993. Mice carrying null mutations of the genes encoding insulin-like growth factor-1 (IGF-1) and type 1 IGF receptor (IGF1R). Cell 75, 59-72.

Liu, Z.H., Xu, J.S., Colvin, J.S., Ornitz, D.M., 2002. Coordination of chondrogenesis and osteogenesis by fibroblast growth factor 18. Genes & Development 16, 859-869.

Long, F.X., Joeng, K.S., Xuan, S.H., Efstratiadis, A., McMahon, A.P., 2006. Independent regulation of skeletal growth by Ihh and IGF signaling. Developmental Biology 298, 327-333.

Loomes, K.M., Stevens, S.A., O'Brien, M.L., Gonzalez, D.M., Ryan, M.J., Segalov, M., Dormans, N.J., Mimoto, M.S., Gibson, J.D., Sewell, W., Schaffer, A.A., Nah, H.D., Rappaport, E.F., Pratt, S.C., Dunwoodie, S.L., Kusumi, K., 2007. Dll3 and Notch1 genetic interactions model axial segmental and craniofacial malformations of human birth defects. Dev. Dyn. 236, 2943-2951.

Lopezmartinez, A., Chang, D.T., Chiang, C., Porter, J.A., Ros, M.A., Simandl, B.K., Beachy, P.A., Fallon, J.F., 1995. Limb patterning activity and restricted posterior localization of the amino-terminal product of Sonic Hedgehog cleavage. Current Biology 5, 791-796.

Louvi, A., Grove, E.A., 2011. Cilia in the CNS: The Quiet Organelle Claims Center Stage. Neuron 69, 1046-1060.

Lu, Q.H., Yan, J., Adler, P.N., 2010. The Drosophila Planar Polarity Proteins Inturned and Multiple Wing Hairs Interact Physically and Function Together. Genetics 185, 549-U1603.

Macica, C., Lian, G., Nasiri, A., Broadus, A.E., 2011. Genetic Evidence of the Regulatory Role of Parathyroid Hormone-Related Protein in Articular Chondrocyte Maintenance in an Experimental Mouse Model. Arthritis and Rheumatism 63, 3333-3343.

Maeda, Y., Nakamura, E., Nguyen, M.T., Suva, L.J., Swain, F.L., Razzaque, M.S., Mackem, S., Lanske, B., 2007. Indian Hedgehog produced by postnatal chondrocytes is essential for maintaining a growth plate and trablecular bone. Proceedings of the National Academy of Sciences of the United States of America 104, 6382-6387.

Magoffin, D.A., 2005. Ovarian theca cell. The international journal of biochemistry & cell biology 37, 1344-1349.

Mak, K.K., Bi, Y.M., Wan, C., Chuang, P.T., Clemens, T., Young, M., Yang, Y.Z., 2008a. Hedgehog signaling in mature osteoblasts regulates bone formation and resorption by controlling PTHrP and RANKL expression. Developmental Cell 14, 674-688.

Mak, K.K., Kronenberg, H.M., Chuang, P.-T., Mackem, S., Yang, Y., 2008b. Indian hedgehog signals independently of PTHrP to promote chondrocyte hypertrophy. Development 135, 1947-1956.

Martinez-Cerdeno, V., Lemen, J.M., Chan, V., Wey, A., Lin, W.C., Dent, S.R., Knoepfler, P.S., 2012. N-Myc and GCN5 Regulate Significantly Overlapping Transcriptional Programs in Neural Stem Cells. PLoS One 7.

Maruyama, Z., Yoshida, C.A., Furuichi, T., Amizuka, N., Ito, M., Fukuyama, R., Miyazaki, T., Kitaura, H., Nakamura, K., Fujita, T., Kanatani, N., Moriishi, T., Yamana, K., Liu, W., Kawaguchi, H., Komori, T., 2007. Runx2 determines bone maturity and turnover rate in postnatal bone loss in estrogen deficiency. Dev. Dyn. 236, 1876-1890.

Meyer, N.P., Roelink, H., 2003. The amino-terminal region of Gli3 antagonizes the Shh response and acts in dorsoventral fate specification in the developing spinal cord. Developmental Biology 257, 343-355.

Mfopou, J.K., Baeyens, L., Bouwens, L., 2012. Hedgehog signals inhibit postnatal beta cell neogenesis from adult rat exocrine pancreas in vitro. Diabetologia 55, 1024-1034.

Minina, E., Kreschel, C., M.C., N., Ornitz, D.M., Vortkamp, A., 2002. Interaction of FGF, Ihh/Pthlh, and BMP signaling integrates chondrocyte proliferation and hypertrophic differentiation. Developmental Cell 3, 439-449.

Moumen, M., Chiche, A., Deugnier, M.A., Petit, V., Gandarillas, A., Glukhova, M.A., Faraldo, M.M., 2012. The Proto-Oncogene Myc Is Essential for Mammary Stem Cell Function. Stem Cells 30, 1246-1254.

OMIM, 2013. Online Mendelian Inheritance in Man (OMIM). Mckusick-Nathans Institute of Genetic Medicine, Johns Hopkins University, Baltimore, MD.

Pan, J.M., Wang, Q., Snell, W.J., 2005. Cilium-generated signaling and cilia-related disorders. Laboratory Investigation 85, 452-463.

Park, T.J., 2008. PCP signaling and ciliogenesis in vertebrate embryos. University of Texas - Austin, Austin, TX.

Park, T.J., Haigo, S.L., Wallingford, J.B., 2006. Ciliogenesis defects in embryos lacking inturned or fuzzy function are associated with failure of planar cell polarity and Hedgehog signaling. Nature Genetics 38, 303-311.

Park, W.J., Liu, J.C., Sharp, E.J., Adler, P.N., 1996. The Drosophila tissue polarity gene inturned acts cell autonomously and encodes a novel protein. Development 122, 961-969.

Parmantier, E., Lynn, B., Lawson, D., Turmaine, M., Namini, S.S., Chakrabarti, L., McMahon, A.P., Jessen, K.R., Mirsky, R., 1999. Schwann cell-derived desert hedgehog controls the development of peripheral nerve sheaths. Neuron 23, 713-724.

Pepinsky, R.B., Zeng, C.H., Wen, D.Y., Rayhorn, P., Baker, D.P., Williams, K.P., Bixler, S.A., Ambrose, C.M., Garber, E.A., Miatkowski, K., Taylor, F.R., Wang, E.A., Galdes, A., 1998. Identification of a palmitic acid-modified form of human Sonic hedgehog. J. Biol. Chem. 273, 14037-14045.

Pierucci-Alves, F., Clark, A.M., Russell, L.D., 2001. A developmental study of the Desert hedgehog-null mouse testis. Biol. Reprod. 65, 1392-1402.

Pola, R., Ling, L.E., Silver, M., Corbley, M.J., Kearney, M., Pepinsky, R.B., Shapiro, R., Taylor, F.R., Baker, D.P., Asahara, T., Isner, J.M., 2001. The morphogen Sonic hedgehog is an indirect angiogenic agent upregulating two families of angiogenic growth factors. Nature Medicine 7, 706-711.

Razzaque, M.S., Soegiarto, D.W., Chang, D., Long, F.X., Lanske, B., 2005. Conditional deletion of Indian hedgehog from collagen type 2 alpha I-expressing cells results in abnormal endochondral bone formation. Journal of Pathology 207, 453-461.

Ribes, V., Briscoe, J., 2009. Establishing and Interpreting Graded Sonic Hedgehog Signaling during Vertebrate Neural Tube Patterning: The Role of Negative Feedback. Cold Spring Harbor Perspectives in Biology 1.

Rida, P.C.G., Chen, P., 2009. Line up and listen: Planar cell polarity regulation in the mammalian inner ear. Semin. Cell Dev. Biol. 20, 978-985.

Riddle, R.D., Johnson, R.L., Laufer, E., Tabin, C., 1993. Sonic-Hedgehog mediates the polarizing activity of the ZPA. Cell 75, 1401-1416.

Rohatgi, R., Milenkovic, L., Scott, M.P., 2007. Patched1 regulates Hedgehog signaling at the primary cilium. Science 317, 372-376.

Ros, M.A., Dahn, R.D., Fernandez-Teran, M., Rashka, K., Caruccio, N.C., Hasso, S.M., Bitgood, J.J., Lancman, J.J., Fallon, J.F., 2003. The chick oligozeugodactyly (ozd) mutant lacks sonic hedgehog function in the limb. Development 130, 527-537.

Ross, A.J., May-Simera, H., Eichers, E.R., Kai, M., Hill, J., Jagger, D.J., Leitch, C.C., Chapple, J.P., Munro, P.M., Fisher, S., Tan, P.L., Phillips, H.M., Leroux, M.R., Henderson, D.J., Murdoch,

J.N., Copp, A.J., Eliot, M.M., Lupski, J.R., Kemp, D.T., Dollfus, H., Tada, M., Katsanis, N., Forge, A., Beales, P.L., 2005. Disruption of Bardet-Biedl syndrome ciliary proteins perturbs planar cell polarity in vertebrates. Nature Genetics 37, 1135-1140.

Saika, S., Muragaki, Y., Okada, Y., Miyamoto, T., Ohnishi, Y., Ooshima, A., Kao, W.W.Y., 2004. Sonic hedgehog expression and role in healing corneal epithelium. Investigative Ophthalmology & Visual Science 45, 2577-2585.

Scherz, P.J., McGlinn, E., Nissim, S., Tabin, C.J., 2007. Extended exposure to Sonic hedgehog is required for patterning the posterior digits of the vertebrate limb. Developmental Biology 308, 343-354.

Shimoyama, A., Wada, M., Ikeda, F., Hata, K., Matsubara, T., Nifuji, A., Noda, M., Amano, K., Yamaguchi, A., Nishimura, R., Yoneda, T., 2007. Ihh/Gli2 signaling promotes regulating Runx2 expression osteoblast differentiation by and function. Mol. Biol. Cell 18, 2411-2418.

Simpson, F., Kerr, M.C., Wicking, C., 2009. Trafficking, development and hedgehog. Mech. Dev. 126, 279-288.

Smith, P.M., Sim, F.J., Barnett, S.C., Franklin, R.J.M., 2001. SCIP/Oct-6, Krox-20, and desert hedgehog mRNA expression during CNS remyelination by transplanted olfactory ensheathing cells. Glia 36, 342-353.

Song, B., Haycraft, C.J., Seo, H.S., Yoder, B.K., Serra, R., 2007. Development of the post-natal growth plate requires intraflagellar transport proteins. Developmental Biology 305, 202-216.

Spicer, L.J., Sudo, S., Aad, P.Y., Wang, L.S., Chun, S.Y., Ben-Shlomo, I., Klein, C., Hsueh, A.J.W., 2009. The hedgehog-patched signaling pathway and function in the mammalian ovary: a novel role for hedgehog proteins in stimulating proliferation and steroidogenesis of theca cells. Reproduction 138, 329-339.

St-Jacques, B., Hammerschmidt, M., McMahon, A.P., 1999. Indian hedgehog signaling regulates proliferation and differentiation of chondrocytes and is essential for bone formation (vol 13, pg 2072, 1999). Genes & Development 13, 2617-2617.

Stanton, B.R., Perkins, A.S., Tessarollo, L., Sassoon, D.A., Parada, L.F., 1992. Loss of N-myc function results in embryonic lethality and failure of the epithelial component of the embryo to develop. Genes & Development 6, 2235-2247.

Tabin, C.J., McMahon, A.P., 2008. Grasping limb patterning. Science 321, 350-352.

Taipale, J., Cooper, M.K., Maiti, T., Beachy, P.A., 2002. Patched acts catalytically to suppress the activity of Smoothened. Nature 418, 892-897.

Tissir, F., Goffinet, A.M., 2010. Planar cell polarity signaling in neural development. Current Opinion in Neurobiology 20, 572-577.

Tree, D.R.P., Ma, D., Axelrod, J.D., 2002. A three-tiered mechanism for regulation of planar cell polarity. Semin. Cell Dev. Biol. 13, 217-224.

van den Brink, G.R., 2007. Hedgehog signaling in development and homeostasis of the gastrointestinal tract. Physiological Reviews 87, 1343-1375.

Varjosalo, M., Taipale, J., 2008. Hedgehog: functions and mechanisms. Genes & Development 22, 2454-2472.

Varlakhanova, N.V., Cotterman, R.F., deVries, W.N., Morgan, J., Donahue, L.R., Murray, S., Knowles, B.B., Knoepfler, P.S., 2010. myc maintains embryonic stem cell pluripotency and self-renewal. Differentiation 80, 9-19.

Vortkamp, A., Lee, K., Lanske, B., Segre, G.V., Kronenberg, H.M., Tabin, C.J., 1996. Regulation of rate of cartilage differentiation by Indian hedgehog and PTH-related protein. Science 273, 613-622.

Wallace, V.A., Raff, M.C., 1999. A role for Sonic hedgehog in axon-to-astrocyte signalling in the rodent optic nerve. Development 126, 2901-2909.

Wallingford, J.B., Mitchell, B., 2011. Strange as it may seem: the many links between Wnt signaling, planar cell polarity, and cilia. Genes & Development 25, 201-213.

Wang, C.K.L., Tsugane, M.H., Scranton, V., Kosher, R.A., Pierro, L.J., Upholt, W.B., Dealy, C.N., 2011. Pleiotropic Patterning Response to Activation of Shh Signaling in the Limb Apical Ectodermal Ridge. Dev. Dyn. 240, 1289-1302.

Wang, E.M., Wang, J., Chin, E., Zhou, J.A., Bondy, C.A., 1995. Cellular patterns of insulin-like growth factor system gene expression in murine chondrogenesis and osteogenesis. Endocrinology 136, 2741-2751.

Wang, Y.H., Guo, N.N., Nathans, J., 2006. The role of frizzled3 and frizzled6 in neural tube closure and in the planar polarity of inner-ear sensory hair cells. J. Neurosci. 26, 2147-2156.

Wijgerde, M., Ooms, M., Hoogerbrugge, J.W., Grootegoed, J.A., 2005. Hedgehog signaling in mouse ovary: Indian hedgehog and desert hedgehog from granulosa cells induce target gene expression in developing theca cells. Endocrinology 146, 3558-3566.

Wilson, S.L., Wilson, J.P., Wang, C.B., Wang, B.L., McConnell, S.K., 2012. Primary cilia and Gli3 activity regulate cerebral cortical size. Dev. Neurobiol. 72, 1196-1212.

Winnier, G., Blessing, M., Labosky, P.A., Hogan, B.L.M., 1995. Bone morphogenic protein-4 is required for mesoderm formation and patterning in the mouse. Genes & Development 9, 2105-2116.

Wong, L.L., Adler, P.N., 1993. Tissue polarity genes of *Drosophila* regulate the subcellular location for prehair initiation in pupal wing cells. Journal of Cell Biology 123, 209-221.

Wu, G., Huang, X.P., Hua, Y.M., Mu, D.Z., 2011. Roles of planar cell polarity pathways in the development of neutral tube defects. J. Biomed. Sci. 18.

Yang, S., Wang, C., 2012. The intraflagellar transport protein IFT80 is required for cilia formation and osteogenesis. Bone 51, 407-417.

Yao, H.H.C., Whoriskey, W., Capel, B., 2002. Desert Hedgehog/Patched 1 signaling specifies fetal Leydig cell fate in testis organogenesis. Genes & Development 16, 1433-1440.

Yoon, B.S., Lyons, K.M., 2004. Multiple functions of BMPs in chondrogenesis. J. Cell. Biochem. 93, 93-103.

Yoshida, E., Noshiro, M., Kawamoto, T., Tsutsumi, S., Kuruta, Y., Kato, Y., 2001. Direct inhibition of Indian hedgehog expression by parathyroid hormone (PTH)/PTH-related peptide and up-regulation by retinoic acid in growth plate chondrocyte cultures. Experimental Cell Research 265, 64-72.

Young, B., Lowe, J., Stevens, A., Heath, J., 2006. Wheater's Functional Histology, 5th ed. Elsevier, Philadelphia.

Zacharias, W.J., Madison, B.B., Kretovich, K.E., Walton, K.D., Richards, N., Udager, A.M., Li, X., Gumucio, D.L., 2011. Hedgehog signaling controls homeostasis of adult intestinal smooth muscle. Developmental Biology 355, 152-162.

Zeng, H.Q., Hoover, A.N., Liu, A.M., 2010. PCP effector gene Inturned is an important regulator of cilia formation and embryonic development in mammals. Developmental Biology 339, 418-428.

Zhou, Z.Q., Shung, C.Y., Ota, S., Akiyama, H., Keene, D.R., Hurlin, P.J., 2011. Sequential and Coordinated Actions of c-Myc and N-Myc Control Appendicular Skeletal Development. PLoS One 6.

ACADEMIC VITA

RACHEL W. CHANG

·&·

Education

B.S. in Biology – Genetics and Development Option, with Honors | May 2013
The Pennsylvania State University, University Park, PA

Honors and Awards

- Student Marshal for the Eberly College of Science Commencement
  Eberly College of Science, The Pennsylvania State University | May 2013
- John W. Oswald Award for Outstanding Leadership in Scholarship
  Student Affairs, The Pennsylvania State University | April 2013
- Eberly College of Science outstanding student and representative at the Penn State vs. Ohio State football game halftime ceremony honoring academic achievement
  Eberly College of Science, The Pennsylvania State University | October 2012
- Scholar Involvement Award for Outstanding Academic Excellence and Leadership
  Schreyer Honors College, The Pennsylvania State University | September 2012
- Scholar Advancement Team Outstanding Member Award for Commitment and Service
  Schreyer Honors College, The Pennsylvania State University | November 2010
- Evan Pugh Senior Award for Academic Excellence
  The Pennsylvania State University | April 2013
- Evan Pugh Junior Award for Academic Excellence
  The Pennsylvania State University | April 2012
- President Sparks Sophomore Award for Academic Excellence
  The Pennsylvania State University | April 2011
- President's Freshman Award for Academic Excellence
  The Pennsylvania State University | April 2010
- Dean's List
  The Pennsylvania State University | December 2009-May 2013
- Academic Excellence Scholarship
  Schreyer Honors College, The Pennsylvania State University | August 2009-May 2013
- Hammond Memorial Science Scholarship
  Eberly College of Science, The Pennsylvania State University | March 2012
- Undergraduate Research Scholarship
  Eberly College of Science, The Pennsylvania State University | December 2011
- Student Leader Scholarship
  Student Affairs, The Pennsylvania State University | December 2011 & 2012
- Of the Month Local and Regional Award for Outstanding Student Programming Initiatives
  National Residence Hall Honorary | March 2013

Leadership, Service, and Memberships

- Member of the Hershey Medical Center Cardiac Care Mission to Ecuador
  | *November 2012*
- Logistics chair of the Schreyer Honors College Day of Service
  | *September 2009-March 2013*
- Member of the Schreyer Honors College Scholar Advancement Team
  | *December 2009-May 2013*
- Chair of the Schreyer Honors College Founders Day Celebration
  | *April-September 2010*
- Member of the Eberly College of Science Science LionPride Ambassador Group
  | *September 2009-May 2013*
- Presenter and featured student in Schreyer Honors College and Eberly College of Science student recruitment events and promotional material
  | *April 2010-May 2013*
- Violinist in The Pennsylvania State University Orchestras
  | *August 2009-May 2013*
  Section leader | *January 2011-May 2013*
- Violinist in the Rose Tree Pops – Media, PA
  | *Summers 2010-2012*
- Mentor for the Eberly College of Science STEM Career Day for Girls
  | *February 2012*
- English as a Second Language Tutor, Mid-State Literacy Council – State College, PA
  | *September-December 2010*
- Co-founder and organizer of the Sound Garden Music Festival at the Penn State Arboretum
  | *August-December 2009*
- Member of the Phi Kappa Phi Honor Society
  | *February 2012-May 2013*
- Member of the National Residence Hall Honorary
  | *April 2011-May 2013*
- Member of the National Society of Collegiate Scholars
  | *January 2010-May 2013*

Professional Experience

- Schreyer Honors College Scholar Assistant
  The Pennsylvania State University | December 2010-May 2013
  - Lead scholar assistant | *August 2012-May 2013*
  - Collaborated with the Honors College administration, staff, and scholar assistant team to develop and facilitate intellectually engaging student programming
  - Served as a mentor, liaison, and resource for Honors College students
- Developmental Biology Undergraduate Researcher
  The Pennsylvania State University | January 2010-May 2013
  - Investigated the role and function of the mammalian *Inturned* gene in ciliogenesis, Hedgehog signaling, and skeletal patterning during embryogenesis
  - Investigated the genetic basis for the ciliary localization of Gli proteins during mammalian embryogenesis
- Teaching Assistant – Leadership Jumpstart course
  Schreyer Honors College, The Pennsylvania State University | August 2010-December 2012
  - Facilitated classes in Leadership Jumpstart, an honors course that challenges students to evaluate and develop their leadership skills through large-scale, group service projects and reflective writing
  - Advised and provided feedback to students on their service projects, presentations, and written analyses
- Immunopharmacology Research Intern
  Johnson & Johnson Pharmaceutical, Radnor, PA | May-August 2012
  - Utilized animal models of emphysema to evaluate the impact on respiratory function
  - Investigated the potential applications of medical imaging in lung function evaluation
- Nemours Undergraduate Summer Research Scholar – Neurogenetics Research Laboratory
  Alfred I. DuPont Hospital for Children, Wilmington, DE | Summers 2010 & 2011
  - Studied the progression, genetic basis, and reversion of Pelizaeus-Merzbacher disease, a neurological condition characterized by reduced myelination

Professional Presentations

- Mouse PCP Effector Protein Inturned Regulates Skeletal Development
  Undergraduate Research Exhibition
  The Pennsylvania State University, University Park, PA | April 11, 2012
- Ultraviolet Irradiation-Induced Reversion of Pelizaeus-Merzbacher Disease
  Nemours Undergraduate Summer Research Scholars Program
  Alfred I. DuPont Hospital for Children, Wilmington, DE | August 13, 2010

Publications

- Chang, R. (2009, December). A Medical Revolution: The College of Physicians of Philadelphia. In *Literary and Cultural Heritage Map of Pennsylvania.* Pennsylvania Center for the Book. Retrieved from http://pabook.libraries.psu.edu/palitmap/CollPhys.html